Simulation of thermal tests in the climatic wind tunnel CD7 at Scania
Master thesis project in fluid mechanics

Jonathan de Laval - jdl@kth.se / jonathan.de.laval@scania.se

July 28, 2016

The photo on the title page is taken during a winter condition test of a Scania R490 4x2 Streamline truck inside the climatic wind tunnel CD7.

Abstract

The Swedish truck and bus manufacturer Scania has a number of test facilities to support the R&D department and for verification of vehicle properties. The latest addition is the climatic wind tunnel Chassis Dynamometer 7 (CD7) which can fit trucks and buses for full scale testing and maintain temperatures in the range from -35 to 50 degree Celsius in the flow circuit, furthermore it can generate both rain and snow conditions. This means that vehicles can be tested in a controlled and repeatable manner at many critical driving conditions. However, since CD7 is a new facility there is a need to tune and interpret the results generated in the tunnel and translate them to true, on road conditions.

In this project the airflow and temperature distribution in the climatic wind tunnel were studied by means of the CFD solver PowerFLOW based on the Lattice Boltzmann method. As a first step the wind tunnel was simulated empty to check the case set up and to understand the basic flow features in the empty tunnel. In the second step a Scania truck was added to the wind tunnel set up, a truck that also exists as a physical test vehicle at Scania R&D. Thirdly, the same vehicle model was simulated in road like conditions to give a reference for comparison. Lastly, a measurement campaign was performed in the climatic wind tunnel in order to get data for comparison and validation of the simulation results.

Simulation results show that CD7 displays an overestimate of wind tunnel airspeed. To match heat exchanger mass flow and recirculation temperatures at 30 km/h it is shown that CD7 should indicate closer to 35 km/h. At this low speed range 5 km/h has a strong effect on recirculation of hot air into the cooling package which translates to 1 °C increase of air temperature into the charge-air cooler. It also corresponds to an increase of 2 °C of the cooling capacity of the vehicle at 30 km/h. Also the temperature in the front air intake system increases by 3 °C which is also a significant change that could affect the tuning of the engine. One degree Celsius is within the measurement accuracy of a thermal test at Scania.

The simulations at 85 km/h give a corresponding correction of the tunnel velocity around 10 km/h, which means that it is consistently about 10 % off.

The experimental results show conformity with the simulations and also support the claim that CD7 indicates an overestimate of the actual airspeed.

Contents

Nomenclature

Abbreviation	Description
BLRS	Boundary Layer Removal System
CAC	Charge Air Cooler
CD	Chassis Dynamometer
CFD	Computational Fluid Dynamics
CWT	Climatic Wind Tunnel
EGR	Exhaust Gas Recirculation
FAI	Front Air Intake
FCD	Flow Control Device
HPC	High Performance Computing
HVAC	Heating Ventilation Air Conditioning
LBM	Lattice Boltzmann Method
OpR	Open Road conditions
RAD	Radiator
STC	Scania Technical Centre
UTM	Underhood Thermal Management
VTM	Vehicle Thermal Management

Symbol	Description
c_p	Pressure coefficient [-]
p	Static pressure [Pa]
q	Dynamic pressure [Pa]
C_D	Drag coefficient [-]
Q	Volume flow [m^3/s]
T	Temperature [°C/K]
T_{cool}	Cooling capacity [°C/K]
T_{TT}	Top Tank Temperature [°C/K]
U	Airspeed [m/s]
ρ	Density [kg/m^2]

Chapter 1

Introduction

This chapter gives a brief introduction of Scania and the subject of climatic wind tunnels, thermal testing and simulation.

1.1 Background

Scania is a Swedish truck manufacturer, that develops and produces high performance heavy trucks and buses for the transport and logistics industry but also vehicles for mining, construction and other special applications.

Previously vehicle engineers at Scania relied on road testing for validation of vehicle properties. This requires a lot of resources and logistics, shipping the trucks or buses to the test location, e.g. southern countries (Spain) for hot weather performance validation or northern Sweden for winter trials. It is also expensive to fly in engineers, mechanics and support personnel to these remote locations. These operations are also subject to uncontrollable parameters such as weather changes, shifting ambient temperatures, winds and cloudiness causing large variations of the results. Therefore, to allow repeatable tests in a consistent environment climatic wind tunnels are used. Scania has a number of these facilities called Chassis Dynamometer short CD, with different abilities. The latest of these is CD7 which is the subject of this paper. The basic idea is to put a controlled load on the engine and produce headwinds or a surrounding with desired temperature so that measurements of the engine room and other systems can be done consistently between different vehicle models. The predecessor to CD7 is CD5 which can provide wind speeds up to 90 km/h and regulate the air temperature from 5 °C, or 2 °C above outside temperature, up to 55 °C, it has heating but no cooling is available.

Since CD7 is such a new facility, commissioned in 2013, Scania has a need to understand the flow field of the wind tunnel and its effect on the thermal tests performed there. In this quest simulation is an unmatched tool for analysing and visualising the air flow inside the tunnel.

Therefore two master thesis projects were performed in the spring 2016, in order to simulate the climatic wind tunnel (CWT) CD7 at Scania Technical Centre (STC). The

Figure 1.1: The CD7 building at Scania Technical Centre (STC) with preparation halls and support offices.

present study is focused on the thermal aspects of the truck and the other one on soiling tests.

1.1.1 Chassis Dynamometer 7

The climatic wind tunnel at STC studied in this project is known as Chassis Dynamometer 7 (CD7). Seen in figure 1.1 is the facility building with the complete wind tunnel systems, preparation hall and support offices. The facility allows for repeatable testing of vehicle systems in diverse climates and weathers all the year around. The wind tunnel part of CD7 consists of a closed flow loop with heating and cooling systems capable of maintaining a temperature inside the test chamber between -35 to 50 degrees Celsius. The test section is 10 meter wide, 20 meter long and with a nozzle of 3.5×3.7 meters giving the cross section of 13 m^2, visible in top right and bottom left of figure 1.2. It also has a system to control humidity and can produce rain and snow in the main air stream visible in the title page photograph. The main fan, rated at 465 kW, can drive the airflow to 100 km/h. At the end of the nozzle is a scoop in the floor, just before the test section, that ingests the nozzle boundary layer through suction. This Boundary Layer Removal System (BLRS) gives a cleaner flow over the test section floor. There is also a large array of powerful lamps to simulate the effects of solar irradiation on the vehicle systems, see bottom right in figure 1.2. The lights are rated at 1.1 kW/m^2 which is comparable to the solar constant at the earth surface, $1.2 - 1.4$ kW/m^2 depending on latitude. The wind tunnel is furthermore clad with acoustic absorbent to dampen background noise as to allow for acoustic measurements of the truck in operation. It is also equipped with two large steel wings called Flow Control

Figure 1.2: Photos inside the climatic wind tunnel from the measuring campaign. Test truck with city trailer and Prandtl-probe (top left). Truck set up from behind and nozzle (top right). Nozzle, wind tunnel access door and Prandtl-probe (bottom left). Solar lamp array in the wind tunnel ceiling (bottom right).

Devices (FCD) that can be extended into the wind tunnel to guide the flow and allow accurate measurements of yaw-angles and buses normally requiring much larger wind tunnels. A more extensive presentation on design aspects and capabilities is given by Duell & et.al. (2016) and the operating manual Tarnutzer (2013).

1.1.2 Vehicle thermal management

The underhood environment of a truck is governed by the engine power output, cooling assembly, fan and ram-air flow through the grille. By the very nature of internal combustion the engine produces a lot of heat. To protect temperature sensitive components and keep the engine working efficiently the engine compartment is shielded and cooled. The heat is dissipated from the different components by the cooling assembly and by the airflow through the engine compartment. The cooling assembly consists of a set of heat exchangers: oil cooler, condenser, exhaust gas recirculation (EGR) cooler, charge-air cooler (CAC) and the radiator (RAD).

If the temperature rises towards the tolerance levels of the heat sensitive components the engine control system will automatically decrease engine output power to save these

components. This however represents a loss of performance to the customer and therefore the vehicles should be built to avoid that kind of situation. Thermal testing is performed in full scale through open road driving, in the test facilities, chassis dynamometers at STC, and with simulations.

One of the more challenging driving cases is low speed hill climbing at high ambient temperatures with high power demand on the engine and low ram-air pressure into the engine compartment. Therefore this type of operation is necessary to test the performance of a vehicle. At those conditions there are many heat related phenomena that are important to capture accurately in CD7 compared to true driving in open road conditions (OpR). Because of this such a case is used as a starting point for these simulations.

1.1.3 Simulation

When working with CFD-simulations or any finite element method one exploits the computers ability to perform a lot of repeated calculations without tiring. In many of these applications it is also possible to perform independent calculations simultaneously. Therefore, the more processors the quicker you can get the results or the larger and more detailed simulations you can run. This is taken to the extreme with super-computing or High Performance Computing (HPC) where the order of thousands processors are used to perform parallel tasks.

With the increasing computer power available, simulation has become an adequate tool for accurate predictions of properties of real systems, in this case trucks. Simulation allows to early evaluate different concepts with short turn around time. It can then act as a tool to restrict and decide on which concepts that should go to prototyping and be put to model or full scale testing.

In this project the commercial code PowerFLOW developed by Exa is used for the simulations. PowerFLOW is based on the Lattice Boltzmann Method and can be extended with other Exa programs to augment its abilities.

1.1.4 Earlier work

At Scania, Hällqvist (2009) did a parametric study of different engine room design aspects and their influence on cooling performance. The effects of the fan position and fan shroud design on radiator mass flow and cooling capacity was examined.

Through the American truck manufacturer Kenworth together with the software company Exa, Horrigan *et al.* (2007) studied simulations of a scale wind tunnel for drag predictions and compared these with real wind-tunnel tests. They studied blockage effects and how wind-tunnel shape and tunnel ventilation details influenced the results. It was found that increased level of detail, specifically wind-tunnel side vents and corner chamfer, in the simulation model gave better correlation to the experiments.

Also in collaboration with Exa, Hyundai through Cyr *et al.* (2011) did a study on how to produce and compare CFD simulations with a wind tunnel scale model. A comparison was done with two different measurement points on the vehicle, representing high and low

pressure coefficients, c_p, to produce correction factors for the drag coefficient C_D. The method reduced the relative error compared with experimental results on C_D from 0.25 % to 0.14 %.

Together with Chalmers and Volvo, Martini *et al.* (2014) did a study where CFD simulations were compared with full scale testing at NRC in Canada, both on external aerodynamics and cooling performance. The study produced a satisfactory agreement between the CFD and wind tunnel testing but also points to some important discrepancies. The cooling drag displayed a high dependency on the turbulence model used, indicating that the flow through the underhood area or cooling assembly might be badly captured. However the best models showed good agreement on cooling performance with wind tunnel tests. Due to lack of proper and accurate drawings, the sensitivity to small changes of the wind-tunnel geometry was examined and showed to have little effect on the major results.

One year before the current project, Hyvärinen (2015) did a Master thesis project simulating full truck models in a generic wind tunnel based on the LLF tunnel at DNW Marknesse and open road conditions to analyse different blockage corrections with respect to drag. DNW in Marknesse is an aerodynamic wind tunnel large enough for full scale testing of trucks. The work was done with PowerFLOW.

At the same time Ekman & Larsson (2015) did their master thesis project on fan ring exit guide vane optimisation. Also simulating the thermal aspects of the engine compartment but with STAR-CCM+.

Both these works provided valuable insights to the simulation process and the current application.

1.2 Scope

The present study aims to evaluate the airflow and measurements of vehicle properties made in the climatic wind tunnel CD7 at Scania. The report will focus on CFD simulations and wind-tunnel verification. Simulations will be performed of the empty wind tunnel and with a full truck model, including thermal aspects. Truck simulations will also be conducted with open road conditions for comparison.

1.2.1 Truck setup

In the scope of this project two trucks are studied in two different aspects. The real trucks are both shown in figure 1.3, to the left is “Fuego” which is used for the simulations and to the right is “Sorgenfrei”, used for the wind tunnel measurements. This division is caused by vehicle and model availability.

Fuego is a test truck at Scania which has been extensively simulated earlier in other projects and is used again for the simulations in this project. It has well known properties from full scale testing and previous simulations. Vehicle type designation is P450DA4x2MNB which for instance means that it is a P-cab, the smallest cab size in the Scania modular system, with 450 horse powers driving the rear axle (4x2), four wheels out of which 2 are

Figure 1.3: Photographs of test trucks Fuego, small P-cab (left) and Sorgenfrei with the larger R-cab inside CD7 (right).

driven. The P-cab of Fuego is 3.2 m high and 2.6 m wide, the roof air deflector extends upwards to 3.7 m from the ground. It has a 13 litre, inline 6 cylinder engine with exhaust gas recirculation and Euro6 emission classification.

Sorgenfrei is another Scania test truck which was used for the wind-tunnel testing due to vehicle availability. Sorgenfrei has the type designation R560LA4x2MNA which means it has the larger R-cab and a 560 horse power V8 engine, also with rear wheel drive. With the R-cab Sorgenfrei stands 4 m tall and is 2.6 m wide.

The city trailer is a relatively small trailer with a single steering rear axle to allow it to take tight corners in a city environment. Its limited size, 9.0 m long, 2.6 m wide and 3.3 m high makes it good for the CD7 testing. Although a full size trailer would fit, this relatively small trailer is the one mostly used at the CD7 facility.

1.3 Objective

Since the CD7 facility still is relatively new, there is a need to increase the understanding of the tunnel airflow and interpret the results generated. The goal of this study is to, through simulation, visualise and better understand flow phenomena and thermal aspects in and around a truck inside CD7. Also if necessary, evaluate how the results from CD7 can be translated to on-road driving. More specifically:

- Set up and run simulations of CD7 empty. Study flow phenomena and the wind tunnel systems, airspeed indication and BLRS.
- Set up and run simulations of a truck in open road conditions and inside CD7. Study flow phenomena in and around the truck and compare between open road and CD7.
- Verify simulations with wind tunnel tests.

1.4 Delimitations

To keep control of the project some of the initial ambition had to be cut down. The simulations are limited to one truck and one trailer set up which is Fuego with the city trailer. The two different environments studied are the open road conditions and CD7. Two velocities and load cases which are 30 km/h with full load representing the low speed hill climbing and 85 km/h with partial load, which is more representative for highway driving.

A potential follow up study will contain the effect of larger trucks and buses. There is also the possibility to simulate the FCD and study the effects of its position and angle of attack.

Chapter 2

Theory

In this chapter the basic idea of the physics behind the fluid solver is presented together with the assumptions and calculation methods for the other analyses performed.

2.1 The Lattice Boltzmann Method

In Computational Fluid Dynamics (CFD) there are a number of methods available dependent on distinctive assumptions which are suitable for different applications. One often comes in contact with the Navier–Stokes equations which are a set of non-linear partial differential equations which deals with the macroscopic properties of a fluid e.g. velocity, pressure and density as well as temperature when combined with an energy equation. The opposite of this continuum approach is particle or molecular dynamics which track the motions and interaction of single particles. This can be done with simple Newtonian mechanics, ordinary differential equations, but the sheer amount of particles present in any lower atmospheric application prohibits any larger scale implementation.

The Lattice Boltzmann Method (LBM) is said to operate between those two on what is called meso–scale, illustrated in figure 2.1. Instead of considering fluid properties or individual particles, LBM is computing distribution functions f, describing position $\bar{r}$ and

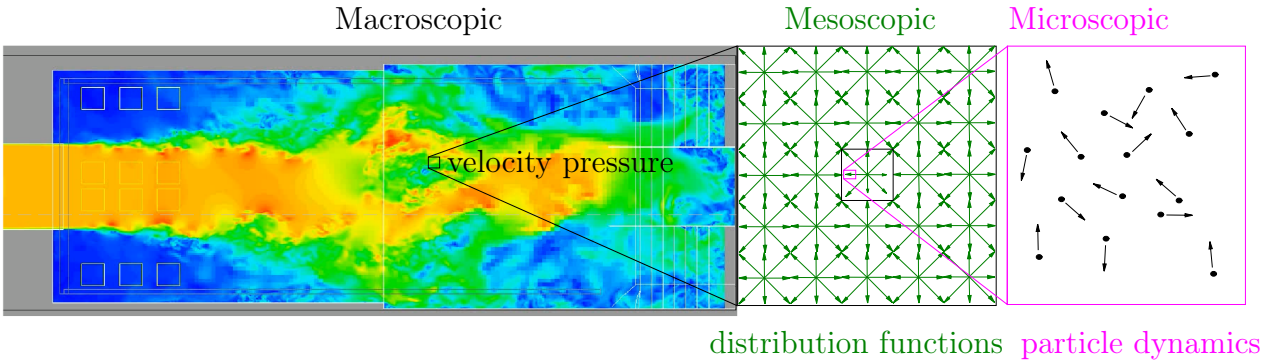

Figure 2.1: Illustration of the different conceptual size scales.

velocity $\bar{c}$, of a set of particles at time t, their phase space

$$f(\bar{r}, \bar{c}, t). \tag{2.1}$$

Physical space is discretised in a lattice of e.g. rectangles, triangles or cubes and for each node in the lattice a set of discrete velocity vectors $\bar{c_i}$ are instantiated, in figure 2.1 a two dimensional, nine velocity grid is illustrated (a scheme called D2Q9, $\bar{0}$ is also counted). Each vector is associated to a particle distribution function f_i and by applying statistical moments to these distribution functions the macroscopic properties such as velocity and density can be calculated at each node e.g.

$$\rho = \sum_i f_i(\bar{r}, t), \tag{2.2}$$

$$\bar{u} = \frac{1}{\rho} \sum_i \bar{c_i} f_i(\bar{r}, t). \tag{2.3}$$

One iteration consist of the transfer or streaming of particle distribution functions to neighbouring nodes and the effects from collision of particles. The changes of the particle distributions are thus calculated by the discretised equation

$$f_i(\bar{r} + \bar{c_i}\delta t, t + \delta t) = f_i(\bar{r}, t) + \Omega_i, \tag{2.4}$$

where δt is a discrete time step during which the particles move to the neighbouring nodes and Ω_i is a collision operator that account for the change of f_i due to collision between particles.

The simplest collision model is the BGK approximation

$$\Omega_i = -\frac{\delta t}{\tau}(f_i - f_i^{eq}), \tag{2.5}$$

that assumes the fluid is reaching an equilibrium distribution f_i^{eq} after a relaxation time τ, e.g the Maxwell–Boltzmann distribution of the fluid. Mass and momentum conservation is ensured by the particle distribution functions streaming between the nodes and by the collision operator which has to satisfy

$$\sum_i \Omega_i = 0, \qquad \sum_i \Omega_i \bar{c_i} = 0. \tag{2.6}$$

A comprehensive description of LBM and coding examples is given by Mohamad (2011) and a derivation of LBM from its predecessor the Lattice Gas Automata is described by Chen & Doolen (1998). Another introduction of LBM is given by Inamuro (2006) together with some examples of implementations. The software provider Exa (2016) has a conceptual description of their implementation but since it is a commercial code all deeper details of the program are unavailable.

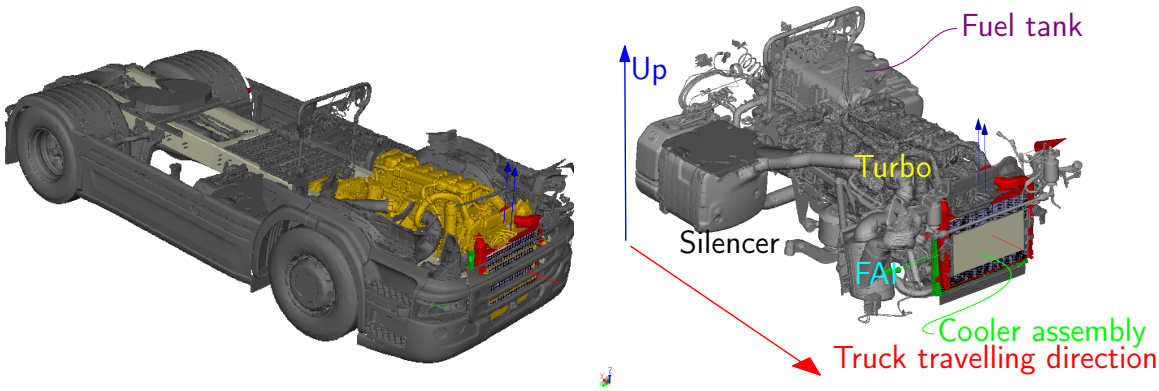

Figure 2.2: Thermal engine model is shown in yellow inside the truck without the cab (left) and only the thermal model is shown with the CAC frame in red and RAD frame in green (right).

2.2 Thermal simulation – Engine model

To accurately evaluate the underhood environment, thermal radiation and conduction have to be included in the simulation model. This is done with an extra thermal solver, PowerTHERM, that works in tandem with the fluid solver. After the fluid solver is initialized the thermal solver takes the convective flow data and calculates the conduction and thermal radiation to calculate the temperature which is then sent back into the fluid solver. This procedure is repeated throughout the whole simulation. The thermal model is shown in figure 2.2 with the cooling assembly visible on the front of the engine with the Charge Air Cooler (CAC) frame in red and radiator (RAD) frame in green. The coordinate systems of the heat exchanger models are also visible with red and blue arrows. The truck enclosing this engine has its cab just above the cylinder heads and is heading down and to the right of the paper. Note in the picture also the level of detail kept for the simulations, tubing, hoses and even electrical wires. Also indicated in the picture is the front air intake (FAI), turbo, silencer and fuel tank. The silencer installation also contain the after treatment system for the exhaust gases. Through the FAI system air is sucked into the compressor side of the turbo, through the CAC, through the engine and collected by the exhaust manifold where it is led to the turbine side of the turbo, into the silencer and after treatment system and finally through the exhaust pipe. Fluid elements are arranged in one dimensional strings to simulate the pipe flow and heat transport through the pipe and pipe material, this together with the external air flow around the engine give the surface temperatures used to calculate the radiation and conduction. The boundary conditions for this model are set as temperatures for the engine block and in the first upstream fluid element for each of the hot pipes around the engine. The temperatures are given by full scale tests of the load case at Scania.

To simulate the heat exchangers and grilles a model with porous media from PowerCOOL is used. Instead of resolving the stack of metal plates and pipes of a heat exchanger, which is expensive, a block of porous media with corresponding flow constraints is used. To get

the effects of a heat exchanger it also takes a coolant mass flow through the heat exchanger and temperature or heat rejection to calculate the coolant temperature including the top tank temperature and the fluid temperature as it exits the porous media. The parameters are again given from full scale tests.

One measure of cooling performance is the cooling capacity

$$T_{cool} = T_{TT} - T_{amb}, \tag{2.7}$$

which is the difference between radiator inlet temperature also called top tank temperature, T_{TT}, and ambient temperature T_{amb}. This is often used as a benchmark when tested at the described load case at 30 km/h and high engine power.

Another important measure is the amount of recirculating air that has already passed the cooling assembly but is forced around to pass again. This is indicated by increased temperature on the inlet surface of the CAC measured by the "Pcool" temperature probes, defined in 3.6.1. It is also indicated in the simulations when streamlines seeded behind the cooling assembly, behind the fan, can be seen going around the frames of the cooling assembly and into the heat exchangers again.

2.3 Wind tunnel systems and experiments

A general description of the climatic wind tunnel CD7 at Scania is given in the Introduction, 1.1.1, and is complemented here with details about relevant subsystems. The complete airline is shown in figure 2.3 with the major parts indicated. The corner enumeration, which starts after the test section or plenum, is shown, the heat exchanger (HX) and main fan located in the elevated return channel are also indicated. Not indicated is the access door to the preparation hall which is located in the rear wall of corner 1.

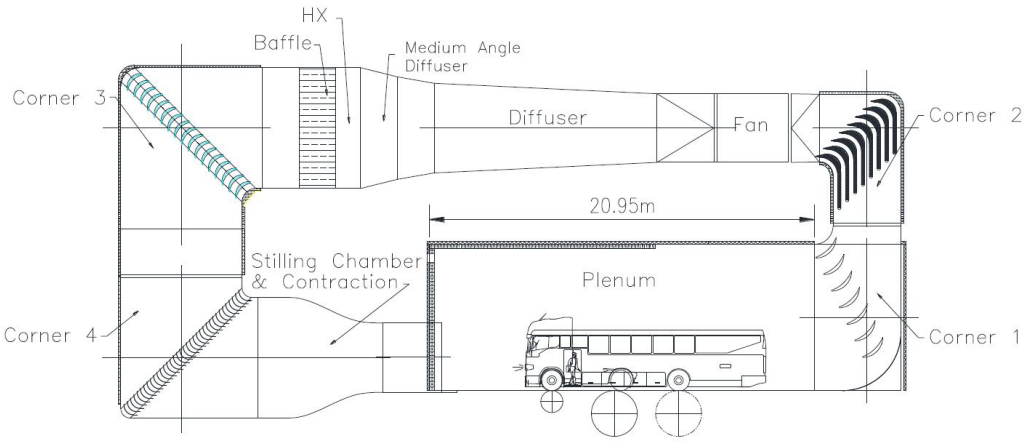

Figure 2.3: Sketch of the CD7 airline with the position of the main fan, heat exchanger and test section indicated.

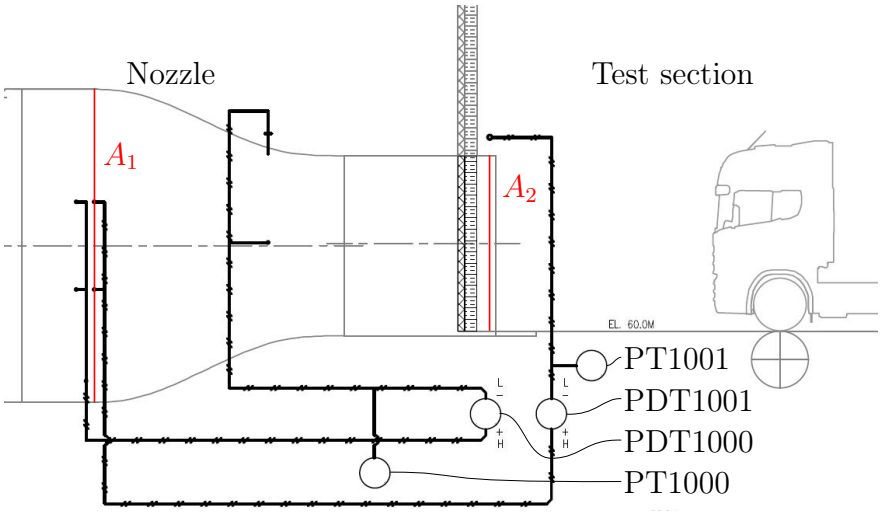

Figure 2.4: Pressure port and cross section locations together with the coupling of the wind tunnel air speed measurement system, crop of the wind tunnel drawing I-010 (2013).

2.3.1 Airspeed measurement

The wind tunnel measures the airspeed through static pressure ports before the nozzle, inside the nozzle and in the test section. The connections and location of the pressure ports are displayed in figure 2.4 which is a crop of the drawing I-010 (2013) depicting the settling chamber, nozzle and a part of the test section with a truck. The PT gauges give an absolute pressure from that port and the PDT gauges are coupled to give the differential pressures between two positions according to the drawing. The two differential pressures are used for two different measuring methods, the nozzle method is connected to PDT1000 and the plenum method to PDT1001. At these low speed airflows the dynamic pressure of the jet can be calculated from the pressure probes with Bernoulli and mass conservation, which for the plenum method give

$$q_2 = (p_1 - p_2) \cdot \kappa = \Delta p \cdot \kappa, \tag{2.8}$$

where

$$\kappa^{-1} = 1 - \left(\frac{A_2}{A_1}\right)^2. \tag{2.9}$$

The areas A_1, A_2 are the cross section areas of the nozzle, shown in figure 2.4, at their respective pressure ports giving the pressures p_1 and p_2. The expression for the nozzle method is slightly different due to the pressure port set up but can be derived in the same fashion. However the commissioning report by JACOBS (2012a) describes how the airspeed indication of the wind tunnel is calculated with the linear function

$$q_{meas} = a \cdot \Delta p + b, \tag{2.10}$$

of the differential pressures, Δp being the value coming from PDT1000 (Nozzle) or PDT1001 (Plenum). The coefficients a and b are calculated to fit the measured dynamic pressure from

Method	a	b	κ
Plenum	1.08	1.15	1.09
Nozzle	1.09	−9.98	1.10

Table 2.1: Calibrated airspeed calculation coefficients and theoretically calculated κ.

a calibration run with a reference probe, JACOBS (2012c). The values of a and b for the measurement methods from the calibration are presented in table 2.1, together with the calculation of κ. For the velocity indication of CD7 this dynamic pressure should then according to the manufacturers own CFD simulations JACOBS (2012a) be blockage corrected with

$$q_{corr} = c_f^2 \cdot q_{meas} \tag{2.11}$$

$$u_{corr} = c_f \cdot u_{meas}, \tag{2.12}$$

where the calibration factor is $c_f = 1.1$. According to the wind tunnel operators the Plenum method is the default setting.

Truck airspeed is challenging to estimate and verify in the wind tunnel in an unambiguous way. Since this is not an aerodynamic wind tunnel and has a limited cross section there is no free-stream flow. The pressure bubble in front of the truck progress into the nozzle which makes it hard to evaluate what airspeed the truck experiences.The result from Exa and Hyundai through Cyr *et al.* (2011) uses a comparison of regions with high and low pressure coefficients to get correction factors. In this case, especially the thermal aspects do not have the same nice non-dimensional coefficients but the idea of matching two different c_p's is used with a high and a low pressure region. In order to compare and match the experienced airspeed between open road and wind tunnel simulation the surface average of the total pressure p_{tot} on the truck windscreen is subtracted with the static pressure p_{stat} on the side windows to estimate the dynamic pressure

$$q_{est} = p_{tot} - p_{stat}, \tag{2.13}$$

the truck experiences. The surface pressures used are shown in figure 2.5 and in some sense makes the whole truck into a large Prandtl-probe.

The airspeed of measurement points in CD7 will be taken with a Prandtl-probe. To calculate the velocity U inside the wind tunnel from the experiments incompressibility is assumed, hence the dynamic pressure q relates to velocity as

$$q = \frac{1}{2}\rho U^2, \tag{2.14}$$

which when solved for U gives

$$U = \sqrt{\frac{2q}{\rho}}, \tag{2.15}$$

Figure 2.5: Estimation of truck dynamic pressure from windscreen and side window pressure averages.

where the density ρ is calculated from the wind tunnel static pressure p, temperature T and the specific gas constant R for air, through the ideal gas law and the dynamic pressure q is the measured differential pressure from the Prandtl-probe.

Another measure used for wind tunnel verification is the pressure coefficient which is defined as

$$c_p = \frac{p - p_\infty}{q}. \tag{2.16}$$

2.3.2 Boundary Layer Removal System

In the nozzle floor there is a scoop with suction to remove the boundary layer of the nozzle. The wind-tunnel manufacturer JACOBS (2012b) calculated the necessary volume flow suction Q of the Boundary Layer Removal System (BLRS) by estimating the volume projected by the scoop in the nozzle floor as a function of airspeed. This is connected to the airspeed measurement Δp in the wind tunnel with the logarithmic equation

$$\ln Q = m \ln \Delta p + b + b' \tag{2.17}$$

where m and b are coefficients identified by a calibration run and b' is an arbitrary constant chosen with experience from other facilities to ensure that the BLRS ingest the whole boundary layer. The coefficients from the calibration of CD7 are displayed in table 2.2. For the simulations Q is multiplied with the density to calculate the mass flow required for the boundary condition of the suction and inlet surface in the model.

Coefficient	m	$b + b'$
Value	0.506	7.787716

Table 2.2: Calibrated BLRS calculation coefficients.

Chapter 3

Simulation setup

The idea of simulation is to take something known (in space or time) and through knowledge of the system calculate something that was unknown somewhere or sometime else.
This chapter gives a presentation of the computer resources used in this project and describes the simulation models that are used and the case set up with the pre- and post-processing tools.

3.1 Resources

The computing resources used in this work are supplied by Scania and KTH PDC.

3.1.1 Workstation

For pre- and post-processing of the simulations a local workstation supplied by Scania is used. The computer is a DELL Precision T7600 with a 16 core Intel Xeon E5-2643 processor at 3.30 GHz. It has 128 GB of RAM and a Nvidia Quadro 5000 graphics card. It is running with a Red Hat Enterprise Linux (RHEL), (Release 6.7 Santiago).

3.1.2 Cluster at KTH PDC

With support from the Swedish National Infrastructure for Computing (SNIC) "Parallelldatorcentrum" (PDC) at KTH maintain a supercomputer for academic research and industrial cooperation. It's a Cray XC40 system consisting of 9 racks containing 1676 nodes which sums up to 53632 cores with a peak performance at 1.9 petaflops. At commission November 2014 this gave it position no. 32 in the TOP500 list of worldwide supercomputers but in the latest list, November 2015, it has slipped down to a still impressive position 51, www.top500.org.

3.1.3 Clusters at Scania

Locally Scania users also have disposal of various computer clusters for running heavy calculations. One of the systems used in this project is based on Intel Xeon processors with 20 cores and 64 GB of RAM per node, running with RHEL 6.4.

3.2 Software

The simulations are performed with Exa's PowerFLOW suite. The preprocessor is called PowerCASE and it manages the different setups of models and configurations such as boundary conditions, physics and coupling to the thermal models. The fluid solver PowerFLOW allows large scale parallelisation and has been tested by Scania to more than 1e4 cores with good scalability. To get reasonable turn around times all simulations are performed on clusters with at least 1e3 cores. PowerTHERM and PowerCOOL work in tandem with the PowerFLOW solver and calculates the thermal parts. PowerTHERM takes on conduction and radiation in the areas specified by the thermal model, see figure 2.2 whilst PowerCOOL calculates the interaction with the heat exchangers, CAC and RAD. The Post-processor PowerVIZ is used to read the generated data and prepare flow visualisations in animations, planes and tables for analysis. Also available are small scripts accessed through the terminal for generating data tables which are readable with text editors and plot programs. Octave and GNUplot are used to post process these raw-data tables into plots for presentations and the report.

3.3 Models

All models and geometries were given as NASTRAN or STL files which could be imported and put together for the different cases in the pre-processor PowerCASE.

3.3.1 Truck set up

The details of the truck Fuego is given in 1.2.1 and the simulation model, taken from earlier simulations, is shown in figure 3.1. The red surface on the exhaust marks the definition of a fluid inlet to simulate the exhaust gases and the blue fields on the front represent the porous media to model the steel mesh of the grille. The red arrows are axle definitions for the rotating surfaces simulating the wheel rotation, the red axle of the fan is also visible sticking out of the front grille. Note also all the fine details kept for the simulations e.g. wind screen wipers, hydraulic hoses and mud guards which are needed to accurately predict the flow and temperature distributions in the engine bay.

The city trailer simulation model with its relatively short length, 9 m, and single wheel pair can be seen in figure 3.2, note again the level of detail of the models. The figure also show as a red arrow the axle definition for the rotating surfaces of the wheels.

3.3.2 Simulation environments

To get open road conditions a large volume is required to avoid blockage effects and wall interference. A sliding wall with the truck velocity is used to simulate the ground motion. The open road "wind tunnel" is shown in figure 3.3. the whole simulation volume is a $180 \times 140 \times 90$ m box.

Figure 3.1: The Fuego model for simulation with details such as axle definitions in red lines and porous media for the grille in blue.

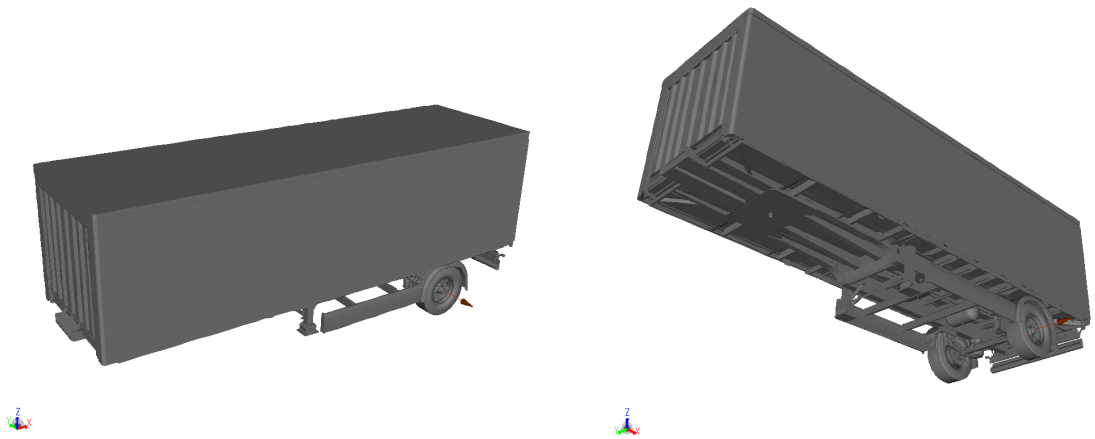

Figure 3.2: The city trailer model for simulation, the arrow represent the axle definition for the rotating surfaces of the wheels.

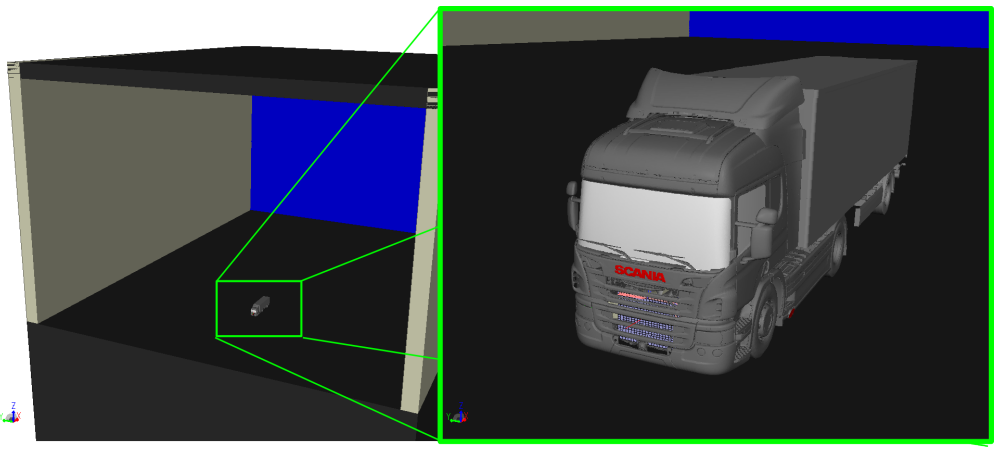

Figure 3.3: Pictures of the open road "wind tunnel", the large volume is necessary to reduce blockage effects.

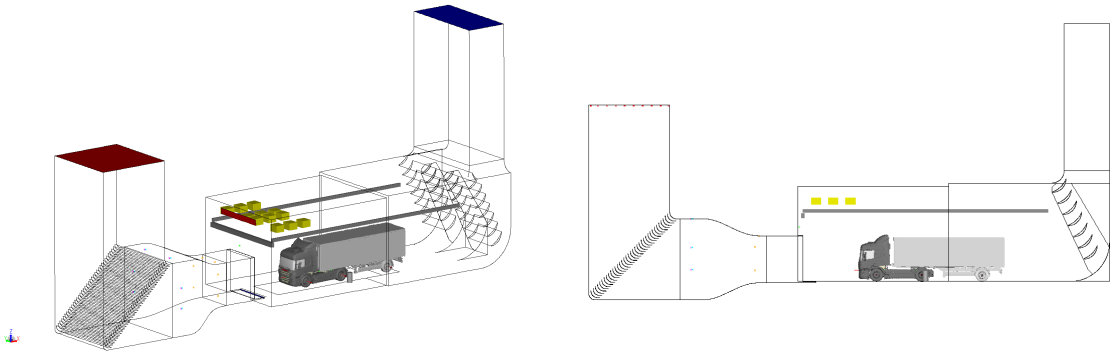

Figure 3.4: The CD7 model with the truck Fuego for simulation. Corner 4 can be seen to the left, upstream of the test section. Fuego is put in the standard position in the test section. Behind the trailer is corner 1 which collects the air flow and directs it upwards back to the fan.

The CD7 simulations are performed with a simplified geometry of the wind tunnel, the return channel together with the main fan on top of the test section is left out but the bottom corners are kept together with their guide vanes. To catch the potentially important intricacies of the flow at the ceiling, the crane and solar array are modeled. The model is shown in figure 3.4 and contains from left to right: Corner 4 with guide vanes, Nozzle, Test section and Corner 1 with the collector guide vanes. The extensions for the inlet (red) and outlet (blue) are part of good practice made to minimise the influence of the inlet and outlet boundaries. The other red area, just above the nozzle, is the BLRS outlet, (fluid inlet) for returning the air sucked out through the BLRS inlet (fluid outlet), marked in blue at the nozzle threshold. The yellow boxes in the ceiling above the truck represent the solar array and the grey long beams represent the crane. Fuego is placed inside the test section of the wind tunnel in the standard position with the front wheels on the rollers 6 m downstream of the nozzle and with zero yaw angle.

3.3.3 Load cases

Two load cases were run, first the benchmarking case at 30 km/h and full engine load with corresponding temperature boundaries for the engine model. The second case is a more common load case representative of highway driving at 85 km/h with corresponding engine load and temperatures. The fan is also working differently between the cases, with full load and low speed the fan is set to maximum at 1544 rpm to maintain airflow through the cooling assembly. At 85 km/h this is not as necessary due to the increased ram air pressure, thus the fan is idling and only rotating with 242 rpm.

3.4 Boundary conditions

The models described above are defined in the solver by their boundary conditions which are described in further detail below.

The most common boundaries are **walls** which is set for all surfaces not defined as something else. Physical walls are the ground, wind-tunnel walls, floor and ceiling as well as truck geometries which are all set with friction and as smooth, i.e. no special surface roughness is defined. The open road simulation uses frictionless walls on the far out "walls" and "ceiling" of the simulation volume.

To simulate the ground motion under the truck a **sliding wall** is used. They are defined by a tangential velocity of the surface and surface roughness for the friction modeling.

To capture the effects from wheel rotation a **rotating wall** condition is used. An axis of rotation is defined in the wheel hub and then an angular velocity and the surfaces describing the wheel are coupled to that. The axis can be seen in figures 3.1 and 3.2. In open road all wheels are spinning over the sliding wall but in CD7 there is no moving belt and there are only rolls for the two wheel pairs of the truck, therefore the trailer wheel rotation is disabled in the CD7 simulations.

In the engine model **thermal boundaries** are used for the simulation of heat generation. Constant temperatures are set in specific points of the engine model in which the conduction through the engine block and internal flow through some of the major components is modeled: air inlet, after the turbo compressor half, exhaust manifold, after the turbo turbine half and into the silencer. The temperatures are taken from experimental data produced at Scania. The ambient temperature of the air is set to $T_{amb} = 25$ °C according to the thermal benchmark test.

For the modeling of inlets and outlets, all surfaces where the fluid enters or exits the volume, one can set a few different conditions. The wind tunnel and open road inlet is set as a **velocity boundary** which for open road conditions is set to the desired airspeed but in CD7 it had to be tuned to give the correct velocity in the test section. The wind tunnel outlet is in both models set as a **pressure boundary** with standard atmospheric static pressure, 101325 Pa. To model the BLRS inlet and outlet its surfaces are set as **mass flows** with the calibrated value 4.7 kg/s at 30 km/h and 15 kg/s at 85 km/h.

The engine air intake and exhaust pipe outlet are also modeled as mass flows. From a

typical driving case the mass flow is set to 0.6 kg/s . In the wind tunnel though the exhaust gases are not released but evacuated by the scavenge system, therefore that boundary is also set as a wall in the wind-tunnel case.

3.5 Grid refinement

The LBM (in PowerFLOW) uses a calculation grid lattice of regular cubes called **Voxels** for fluid elements and **Surfels** for surface elements. They allow for variable resolution to be defined as Volume Refinements (VR) in steps of powers of two times a base size. The standard definition of the VR cell sizes at Scania is given in table 3.1. Regions with large speed variations and areas of special interest are set with finer resolution, VR7-10, while areas with expected uniform bulk flow are set with a coarser grid size, VR4-6, to save computer power. They are used in the open road case to allow for a large simulation volume with low blockage. Some examples of areas with increased resolution are wall boundary layers, the jet shear layer and fine geometries such as the tunnel guide vanes, solar array and especially truck geometries. The Fuego refinement scheme is shown in figure 3.5 with VR6 in light blue encompassing the whole truck, VR7 in green, VR8 in orange just around the tractor and VR9 in dark blue around truck details such as truck corners, mirrors, air deflector and the splitline between the chassis and cab. In the engine compartment one can see the VR8 region in orange and the VR9 region in dark blue and VR10 in pink around the fan blades. The coarsest regions VR0-4 are all outside the CD7 wind tunnel model but require a definition by the program.

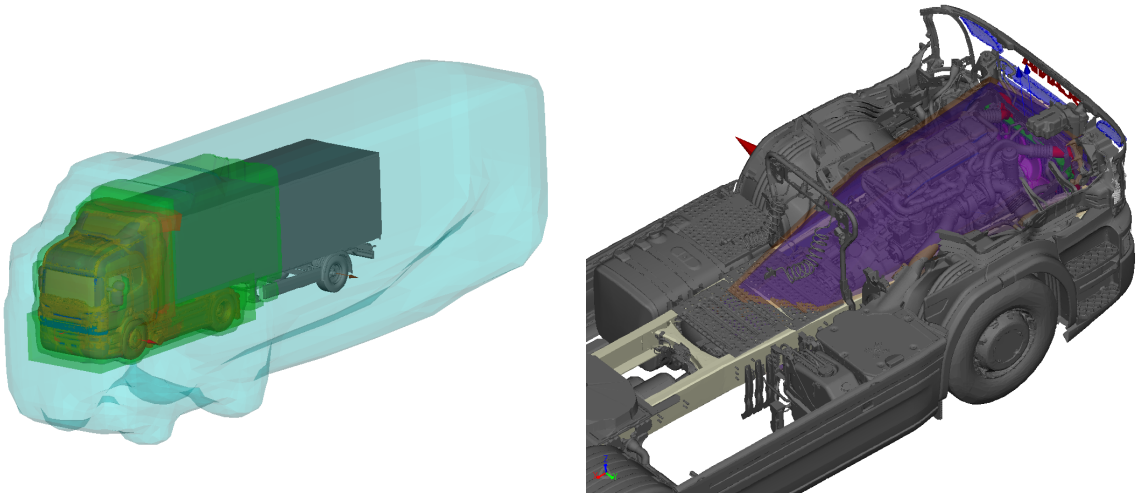

Figure 3.5: Fuego grid refinement scheme, external VR6-9 from light blue, green, orange, dark blue (left) and internal with the CAB hidden it is possible to see the VR8-10 regions in orange, dark blue and pink (right).

Resolution	VR0	VR1	VR2	VR3	VR4	VR5	VR6	VR7	VR8	VR9	VR10
Cell size [mm]	1280	640	320	160	80	40	20	10	5	2.5	1.25

Table 3.1: Definition of the volume refinement regions cell size.

3.6 Simulation measurements

The PowerFLOW simulations are inherently transient and the solver calculates a solution for every grid point and time step but to save performance and storage not all data is stored. In the pre-processor measurements are defined for different regions and surfaces where different data is needed.

3.6.1 Probe measurements

Fluid and surface probes give point measurements either in the fluid or in the points projection to a surface. These can be used to supply high frequency measurements, since they only save point data they can give detailed time history without excessive space requirements. Here they are used to represent real thermal measurement points to give comparable temperature measurements of the engine compartment and as surface probes to simulate the airspeed measurement ports of the wind tunnel.

The probes used around the engine are shown in figure 3.6 which displays the engine installation. The chassis probes "CTL" are marked in green and the pairs visible behind the engine are located on each side of the frame beams. Engine probes "MTL" are in red and the turbo probes "TURBO" are yellow. Recirculation probes "Pcool" on the cooling assembly are also marked in green. The CD7 airspeed indication probes are visible in figures 3.4 and 3.7 which also show the wind tunnel geometry.

3.6.2 Surface measurements

Surface measurements saves the surface components of the fluid e.g. velocity, temperature and pressure distributions. Here this is foremost used to get the pressure distribution on the truck and the temperature on parts around the engine.

3.6.3 Fluid measurements

Fluid measurements give the transient or averaged solution for a defined part of the fluid. In both CD7 and OpR the region in the vicinity of the truck is saved as transient data. For the evaluation of CD7 the whole wind tunnel volume is saved in a 1.5 s average. Thin fluid slices are also saved in interesting cross sections to allow finer measurements with higher sampling frequency without overloading the storage system. Figure 3.7 shows the planes in green for multiple sections of the fluid around and through the truck and in cyan for the planes which intersect the turbo installation. The wind tunnel measurement probes for airspeed indication are also visible marked as crosses and the BLRS inlet and outlet.

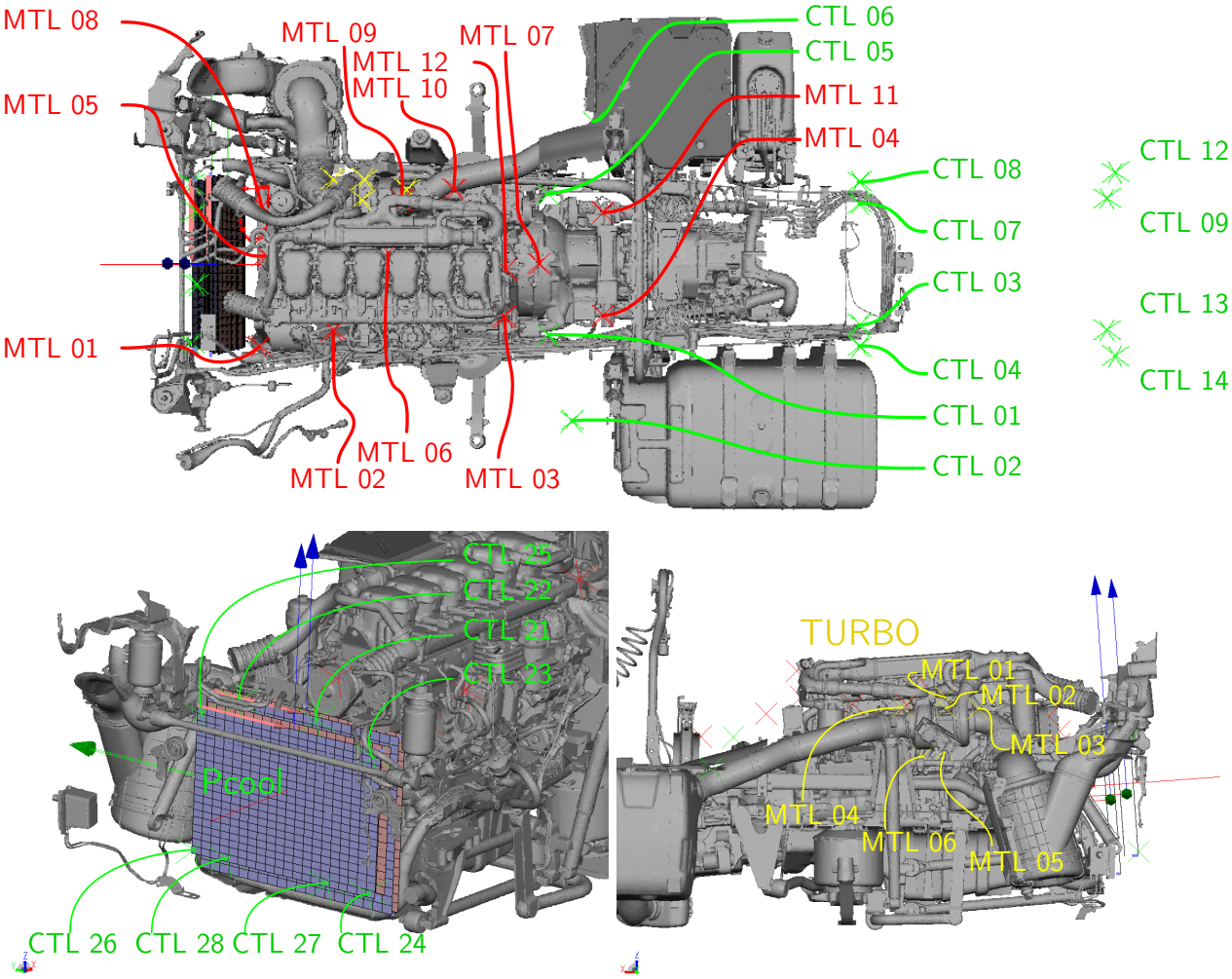

Figure 3.6: Engine probe position definitions. The top view of the engine with the truck facing left show all the engine probes denoted MTL and chassis probes denoted CTL (top). The recirculation probes denoted Pcool CTL can be seen on the front surface of the CAC (bottom left). The turbo probes denoted TURBO MTL are visible on the engines right side (bottom right) the imaginary truck around the engine is facing right. They are all standard measurement points at thermal tests.

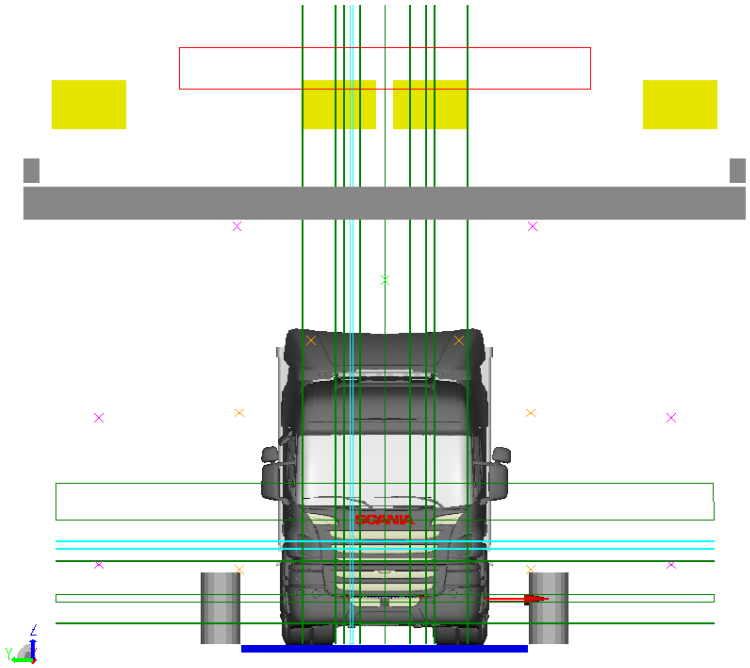

Figure 3.7: Measurement planes for Fuego are shown in green and cyan, the cyan measurements intersect with the turbo. Also visible are some of the CD7 systems, e.g. the surface probes are marked as crosses, the BLRS outlet is visible as a red rectangle and the BLRS suction inlet in solid blue below the truck.

3.7 Convergence

To check if the transient solution has converged, key variables are extracted and studied for oscillations and other fluctuations. Some fluctuations are physical, e.g. turbulent wake vortices and vortex shedding which will never disappear but the nozzle velocity should typically be stable. Here the main indicators are arrays of probes in the inlet, nozzle and outlet together with nozzle velocity, heat exchanger mass flow and temperatures. Mesh convergence is achieved by refining the grid in well chosen regions until the same key parameters do not change between the runs.

Chapter 4

Experimental setup

This chapter presents the available tools and methodology of the wind tunnel measurements. The measurement campaign was performed in the wind tunnel CD7 to verify results from the CFD simulations and to learn more about the wind tunnel systems. A number of soiling tests were also performed for the parallel master thesis project but those results will not be discussed in this paper, see Persson (2016) instead.

4.1 Pressure measurements

To measure the pressures a Prandtl-probe, surface probes, one absolute pressure gauge and one differential pressure gauge were at hand. The pressure probes can be seen in figure 4.1. The Prandtl-probe was mounted on a one meter high strut fastened to a steel plate, which weight was enough to keep it stable and stationary during the wind tunnel operations. The probe extended 1 meter forward from the strut to avoid interference on the pressure ports. For wind-tunnel velocity measurements the absolute gauge was connected to the static pressure port of the Prandtl-probe and the differential gauge between the static port and the total port of the Prandtl-probe, giving the dynamic pressure. For surface measurements the absolute gauge was still connected to the static port of the Prandtl-probe, now located

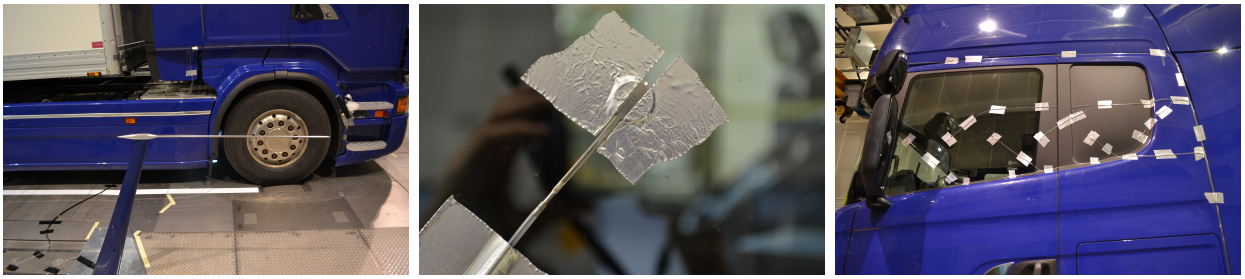

Figure 4.1: Photographs of the Prandtl-probe in position beside the truck (left) and a single surface probe on the side window (middle) and the line of surface probes with pressure tubes drawn with an angle backwards on the side window (right).

in front of the truck, without entering the nozzle, and the differential gauge was connected to the surface pressure probes and the static pressure port of the Prandtl-probe.

4.2 Tunnel points

To verify the simulation a set of points in the wind tunnel, shown in figure 4.2, was measured with the Prandtl-probe to give pressures that could be used to calculate airspeed. In the empty tunnel the middle line was measured with six points "o1-6" and four lateral points "x1-4". This was also done with the truck inside the wind tunnel, the points not blocked by the truck were measured again and two more lateral points "x5-6" were added outside the previous. For each point with and without truck the wind tunnel was run at 15, 30, 50, 70, 85 and 90 km/h. The Prandtl-probe was moved to the different positions inside the wind tunnel and the velocity sweep was performed at each of them. The measured positions are also defined in Appendix A.1.

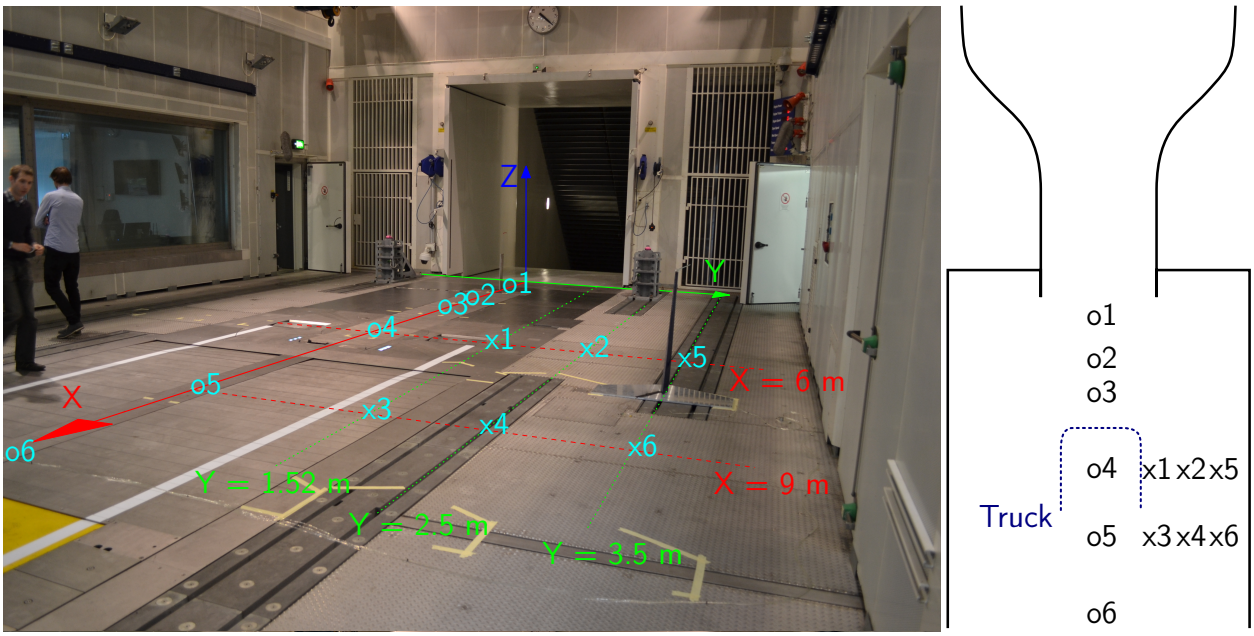

Figure 4.2: Photograph of the empty wind tunnel with the measurement positions marked (left) and a schematic viewed from above (right).

4.3 Truck surface pressure

Another method to verify the simulations and especially truck interaction is to measure surface pressures. Surface pressure probes were attached to the truck at 2400 mm above the ground on the windscreen and side windows, visible in figure 4.1. Three probes were put on the windscreen, one at the centre and two at 500 mm to the left and right. On the side

windows six probes were used at each side, the first one at 170 mm from the forward door frame and then backwards every 250 mm. From this a c_p line can be calculated giving a proper non-dimensional comparison between measured airspeeds and the simulations. This was only done at 30, 75 and 90 km/h due to time constraints.

4.4 Flow visualisation

A thin, 10 mm wide and 0.2 m long, textile ribbon on a 1 m long stick was used to visualise the flow characteristic around the truck and in the chosen measurement points.

Using the rain system and the powerful solar lamps droplets could be tracked optically, visualising some of the larger scale flow phenomena.

For the soiling tests the rain system was tinted with a fluorescent agent making the water glow bright blue under UV illumination. This also offered a way to study flow phenomena around the truck beside the soiling aspects.

4.5 Cooling performance

No thermal tests were performed due to the extensive preparations required and time constraints. Beside that, its usefulness for thermal comparisons is questionable because of the completely different engine installation of the trucks. Sorgenfrei which was available for the wind tunnel experiments has a large V8 engine and Fuego, used in the simulations, has the smaller inline 6 cylinder engine.

Chapter 5

Simulation results

In this chapter a selection of the results from the simulations is presented. The simulations generated vast amounts of data so only a small extract of what has been studied can be presented here.

5.1 Simulation list

The simulations required some iterations for velocity tuning, model and mesh refinements. They are listed in table 5.1 with inlet boundary condition that controls the airspeed and the voxel and surfel count together with an indication of the the truck refinement scheme and a short description. First, to test the model set up and program features the wind tunnel was simulated empty "CD7 empty 30" at 30 km/h as to prepare for the full load case. Then the simulation with open road conditions at 30 km/h was done. The first simulations "CD7

Name	Inlet BC [m/s]	Voxels [10^6]	Surfels [10^6]	Mesh scheme	Description
CD7 Empty 30	2.21	410	23.4	-	Start up, Velocity tuning.
OpR Fuego 1	8.33	507	37.8	"fine"	1st OpR 30 at km/h.
OpR Fuego 2	8.33	597	46.5	"finer"	Added FAI.
CD7 Fuego 1	2.21	534	59.2	"fine"	1st CD7 simulation with truck.
CD7 Fuego 2	2.30	534	59.2	"fine"	Airspeed tuning.
CD7 Fuego 3	2.36	533	59.4	"fine"	Airspeed tuning, added FAI.
CD7 Fuego 4	2.36	629	67.9	"finer"	$CD7_{ind}$ 35 km/h.
CD7 Fuego 5	2.36	864	83.0	"even finer"	Mesh study.
CD7 Fuego 6	2.11	629	67.9	"finer"	$CD7_{ind}$ 30 km/h.
CD7 Empty 85	5.56	406	23.4	-	$CD7_{ind}$ 84 km/h, empty.
OpR Fuego 85	23.6	597	46.5	"finer"	OpR at 85 km/h.
CD7 Fuego 85	5.56	641	68.0	"finer"	$CD7_{ind}$ 82 km/h.

Table 5.1: Simulation list with inlet boundary condition, element count and truck refinement schemes.

Fuego 1" through "3" were done in order to find the wind tunnel airspeed for which the truck experiences 30 km/h and when this turned out to be at 35 km/h indicated by CD7 the simulation "CD7 Fuego 6" was performed to find out if and what kind of differences appear when CD7 indicates 30 km/h. The mesh refinement scheme was given by earlier simulations at Scania and in "CD7 Fuego 4" mesh independence was investigated by adding further refinement regions to the engine room (VR9) and the whole test section was set to (VR5), called "finer" in the table. This showed that mesh independence had not yet been reached and thus the open road simulation "OpR Fuego 2" was redone with the same truck refinements. Also between "OpR Fuego 1" and "2" as well as "CD7 Fuego 2" and "3" the FAI baffle, which was found missing in the model, was added. The refinement study was continued with "even finer" in "CD7 Fuego 5" which showed a decaying mesh dependency and is described in detail further down. Lastly the simulations at 85 km/h were performed to find possible velocity dependent effects and get results representative to highway driving. Both core hours and calender time prevented velocity tuning at 85 km/h, so only one run in CD7 could be performed with the aim to match indicated velocity.

5.2 Main results

As described in 5.1 a number of simulations were performed with different refinements and configurations to tune the wind tunnel model to desired velocities. Some of the middle stage results are included in their respective chapters but the main results of the final comparable simulations are collected in table 5.2 for comparison. The simulations consist of two reference simulations of open road conditions for each velocity and its corresponding load case together with three runs of CD7. The first run of CD7, "CD7 Fuego 4", is with the estimated dynamic pressure q_{est} tuned to the open road case "OpR Fuego 2", and the second run, "CD7 Fuego 6",

Variable		30 km/h full load			85 km/h partial load	
		OpR	CD7 "tuned"	"native"	OpR	CD7
$CD7_{ind}$	[km/h]	-	34.8	30.9	-	82.4
CD7 nozzle velocity	[km/h]	-	30.1	26.1	-	72.5
q_{est}	[Pa]	61	61	50	520	370
CAC mass flow	[kg/s]	2.95	2.94	2.92	1.56	1.21
RAD mass flow	[kg/s]	3.94	3.93	3.89	2.10	1.65
CAC temp inlet	[°C]	31.1	31.2	32.2	25.0	25.0
outlet	[°C]	49.7	49.8	50.8	40.4	44.2
RAD temp inlet	[°C]	48.7	49.0	50.5	36.6	39.3
outlet	[°C]	87.3	87.7	89.6	81.5	95.5
FAI inlet temp	[°C]	31.2	31.8	35.3	40.1	42.9
Cooling capacity	[°C]	84.9	85.1	87.4	69.0	83.9

Table 5.2: Condensed simulation results at 30 km/h and 85 km/h. The open road simulations are regarded as references to the CD7 simulations.

is with CD7 natively indicating 31 km/h, again time constraints prevented the fine tuning. The third run, "CD7 Fuego 85" was aimed at 85 km/h to represent highway driving but fell short at 82 km/h indicated but some phenomena can still be studied and are described in their own chapters.

The compared parameters are the heat exchanger mass flow and inlet temperatures, which all have a major influence on the cooling performance. Also noted is the FAI temperature which is used to indicate the amount of fresh air delivered to the engine and the cooling capacity which, as explained in 2.2, is an important benchmarking parameter.

When the estimated dynamic pressure is matched to open road conditions at 30 km/h the velocity indication of CD7 is off by 5 km/h. It is also possible to see the sensitivity to airspeed of the FAI temperature and cooling capacity at 30 km/h and that they get closer to open road simulations when the dynamic pressure is matched. At 85 km/h the recirculation around the CAC is completely gone, the inlet temperature is equal to the ambient temperature but there is a large difference in mass flow through both the CAC and RAD, causing the difference in outlet temperatures and cooling capacity. With this point it is also possible to see that the mismatch in indicated velocity is consistently 10 % off, this gives a rather large difference in the dynamic pressure and ram-effects which explains the differences in the cooling assembly.

5.3 Convergence and validation

For validation key parameters from the simulations are studied. In figure 5.1 the time history of the inlet, nozzle and outlet pressure as well as indicated velocity are plotted. The pressure probe arrays registered large oscillations with the period 1.57 s with an initial amplitude of 50 Pa at the inlet probes, this can partly be seen in the nozzle and velocity probes as well. These oscillations are not present in the empty wind tunnel and have been caused by entering the truck into the solution of the empty wind tunnel. Starting the wind tunnel from scratch,

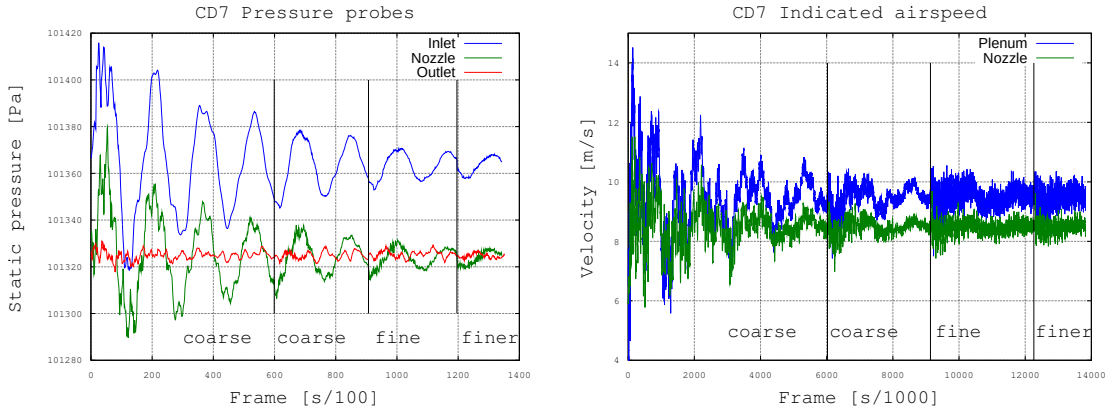

Figure 5.1: Convergence analysis of tunnel parameters with a truck inside the tunnel. Pressure probes in the inlet, nozzle and outlet have registered large oscillations (left). The indicated velocity in CD7 is not as sensitive to the pressure oscillations but subject to noise with the finer discretisation (right).

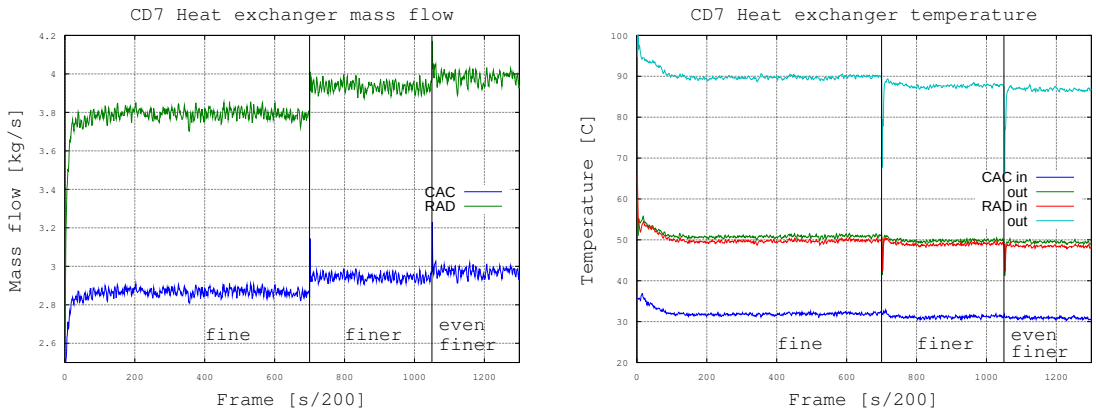

Figure 5.2: Convergence analysis of the truck heat exchanger parameters. CAC and RAD mass flow (left) and their respective inlet and outlet temperatures (right)

without seeding with the solution of the empty wind tunnel, gave much larger oscillations with amplitudes of 1000 Pa. Even though it gives a large disturbance entering the truck in the solution for the empty tunnel the established momentum of the inlet and outlet gives better convergence than a clean start with an empty initial solution. Similar oscillations have also been triggered when changing the inlet boundary condition to tune the jet airspeed. These plots also show no large change in level between the grid refinements which is a good sign of mesh convergence of the external flow. The oscillations are only seen in the indicated velocity during the coarse run and with the switch to "fine" and "finer" discretisation higher noise is registered.

Key parameters for the underhood flow of the truck are the external mass flows through the CAC and RAD as well as their external inlet and outlet temperatures, which are shown in figure 5.2. The data from the coarse simulations are left out because they are done in order to establish an approximation of the external flow field, therefore the resolution is not fine enough to capture the heat exchanger mass flow, giving incorrect engine room flow and temperatures. In the fine runs though they are unaffected by the pressure oscillations seen in the wind tunnel but they do show a dependency on even the fine grid refinements. The final comparison of simulations are done with the "finer" resolution scheme, the "even finer" scheme was done by globally reducing the smallest cell size from 1.25 to 1.1 mm. This simulation shows that the mass flow m through the RAD has still not completely converged, the difference in RAD mass flow

$$\frac{m_{finer} - m_{evenfiner}}{m_{finer}}, \tag{5.1}$$

is around 1 % and the differences seen between the simulations are also of that magnitude. A comparison to open road can be seen in Appendix B.1.

5.4 Airspeed measurements

The simulation of the wind tunnel shows an overestimation of the actual jet velocity by the wind tunnel measurement probes. The calculated velocity indications are presented in table 5.3 together with the inlet boundary condition, the nozzle velocity and the truck estimated dynamic pressure. The nozzle velocity is measured 1 m above the floor and -0.5 m inside the nozzle, which according to the velocity profiles studied in 5.4.2 might be a good free stream estimate. The estimated dynamic pressure overestimates the airspeed but it serves well as a comparison since it is stable and well defined in both simulation environments.

When, in the 30 km/h study, the truck was introduced to the wind tunnel with maintained boundary conditions the airspeed decreased. It was then tuned in "CD7 Fuego 1" through "CD7 Fuego 3" to the comparison point with the estimated dynamic pressure 61 Pa from open road conditions. In "CD7 Fuego 4" when this was combined with the mesh refinement the wind tunnel indicated 35 km/h.

At 85 km/h this tuning of the airspeed could not be performed due to time constraints and the study is limited to CD7 empty, CD7 with Fuego at 82 km/h indicated and Fuego on open road at 85 km/h. It does however show that at both 30 km/h and 85 km/h CD7 overestimates the nozzle velocity with about 10 %, there is also a large difference between the two different measuring methods.

	Velocity [m/s] ([km/h])				
Case	Inlet BC	Nozzle velocity	Plenum	Nozzle	q_{est} [Pa]
CD7 Empty 30	2.21	8.09 (29.1)	9.16 (33.0)	8.31 (29.9)	-
OpR Fuego 30	8.33	-	-	-	61
CD7 Fuego 1	2.21	7.84 (28.2)	8.95 (32.2)	7.86 (28.3)	53
CD7 Fuego 2	2.30	8.16 (29.4)	9.36 (33.7)	8.30 (29.9)	58
CD7 Fuego 3	2.36	8.36 (30.1)	9.62 (34.6)	8.58 (30.9)	62
CD7 Fuego 4	2.36	8.36 (30.1)	9.65 (34.8)	8.62 (31.0)	61
CD7 Fuego 5	2.36	8.37 (30.1)	9.66 (34.8)	8.63 (31.1)	61
CD7 Fuego 6	2.11	7.25 (26.1)	8.59 (30.9)	7.34 (26.4)	50
CD7 Empty 85	5.65	20.0 (71.9)	24.0 (86.3)	22.8 (82.1)	-
OpR Fuego 85	23.6	-	-	-	516
CD7 Fuego 85	5.65	20.2 (72.5)	22.9 (82.4)	23.1 (83.2)	369

Table 5.3: Simulation results of airspeed measurements.

5.4.1 Velocity distribution

As an early evaluation of flow characteristics the velocity distribution is studied in two slices of the fluid. Both go through the nozzle centre, vertically along the centre line of the wind tunnel and horisontally at 1.8 m above the floor or ground. In figure 5.3 the slices of the empty wind-tunnel with indicated velocity 35 km/h (CD7 Fuego 4) and 82 km/h (CD7

Fuego 85) are shown. The wind tunnel jet attaches to the floor and expands outwards, more towards the walls than the ceiling.

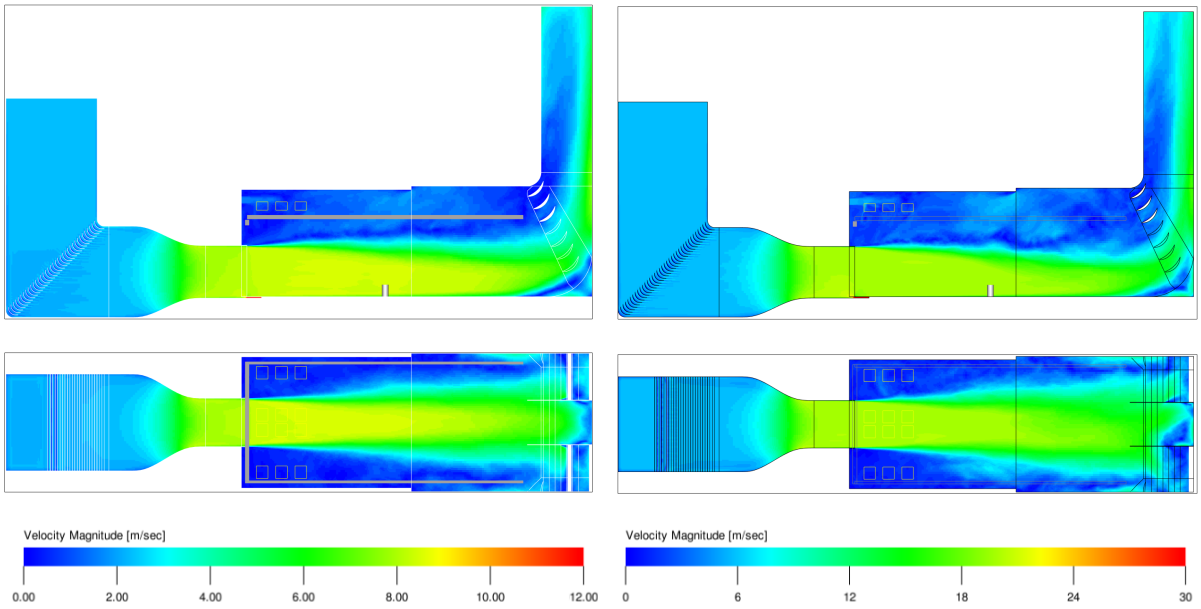

Figure 5.3: Velocity magnitude in central slices (along the centre line and 1.8 m above the floor) of the empty wind-tunnel at indicated velocity 35 km/h and 82 km/h.

Hill climbing – 30 km/h

At the 30 km/h benchmarking case a three second average is shown of the selected slices in figure 5.4. The plots show the test truck Fuego inside the "tuned" wind tunnel (indicating 35 km/h) and in road conditions for comparison. The jet shape of the airflow entering the test chamber in the empty tunnel is disrupted with the truck inside and thrown out to the sides and ceiling. The flow with the truck is not symmetrical which is both due to the asymmetries of the truck, such as the mirrors, chassis components and remaining swirl from the fan, which is working on full power in these simulations. In open road condition one can clearly see the stagnation region in front of the truck and the differences to the wind tunnel field, the flow is properly attached along the trailer and reaches a free stream velocity away from the truck. If one studies the air flow under the truck it is also possible to see how the air close to the ground keeps some airspeed in the open road conditions whilst in CD7 it is stagnant and even reversed in some regions.

In figure 5.5 a flow visualisation with streamlines is shown. The streamlines are seeded just behind the fan in the engine compartment. Despite their internal seed point some characteristic external flow phenomena can be studied. One can clearly see the difference in wheel wake flow which attaches to the ground on open road but is deflected slightly upwards in CD7. It is also possible to see a large scale recirculation of air moving forward close to

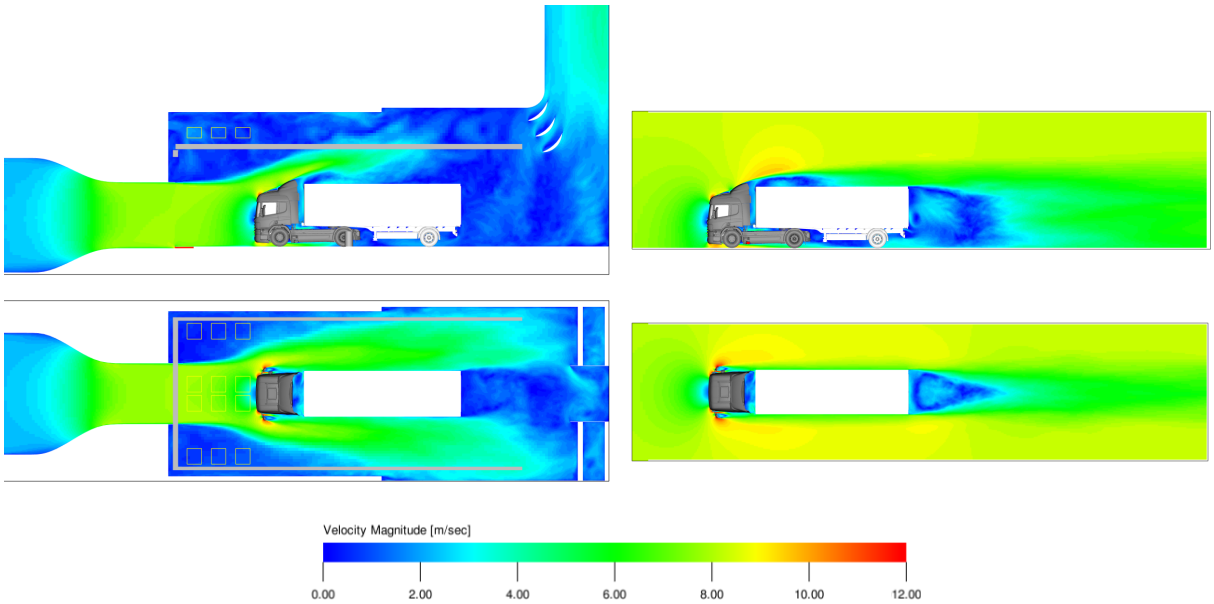

Figure 5.4: Velocity magnitude when simulating 30 km/h in central slices (along the centre line and 1.8 m above the floor), with the truck Fuego in CD7 (left) and Fuego on open road (right).

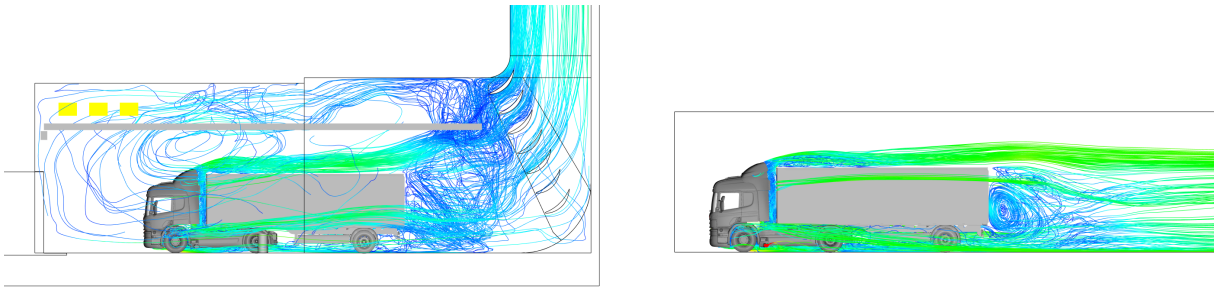

Figure 5.5: Streamlines seeded behind the fan show some differences in flow characteristics between CD7 (left) and OpR (right).

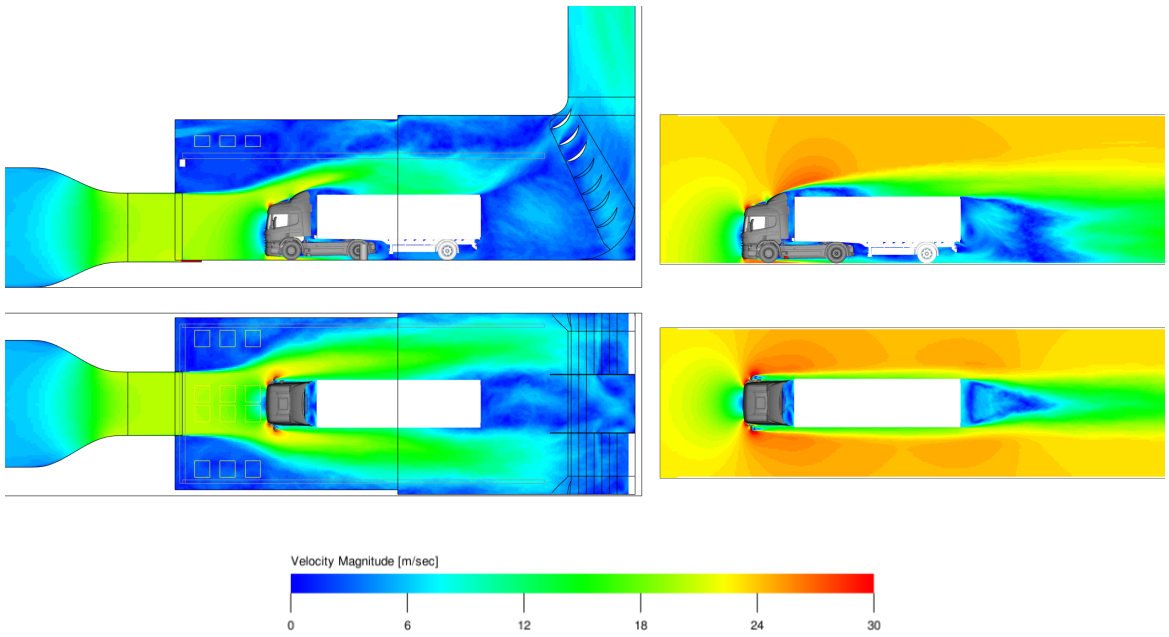

Figure 5.6: Velocity magnitude when simulating 85 km/h in central slices (along the centre line and 1.8 m above the floor) with the truck Fuego in CD7 (left) and Fuego on open road (right).

the ceiling and then fall down in and beside the main jet in CD7. This recirculation has an impact on the temperature distribution in CD7 which is discussed in 5.5.

Highway cruising – 85 km/h

The centre slices are taken out in the 85 km/h cases as well and are shown in figure 5.6. One can see that the airflow maintain attachment further back on the trailer roof at 85 km/h and is much more symmetric along the trailers sides than the 30 km/h simulation. This indicates that the asymmetry at 30 km/h is indeed mainly caused by the fan, which is idling in this case. The large increase in airspeed would also reduce the effects of the fan. The velocity colour scale is the same in both figures so the dramatic difference in colour between CD7 and OpR comes from the mismatch in velocity.

5.4.2 Velocity profile in front of truck

The pressure bubble that builds up on the front of the truck, visible as a bubble shape in the velocity distribution in figures 5.4 and 5.6, is studied by plotting the decrease in airspeed along the wind tunnel centre line, 1 m above ground level, see figure 5.7. In open road this bubble extends about 10 m in front of the truck and it is clearly seen that the wind tunnel jet does not allow the same formation of this bubble. The velocity profiles are shown in figure 5.8 where the x-coordinate is defined from wind tunnel nozzle threshold, shown in figure 4.2 of the tunnel coordinate system. The left plot of figure 5.8 shows the velocity magnitude from the simulations of OpR, CD7 in 30 km/h and 35 km/h which show that the nozzle

velocity is only 26 km/h when 31 km/h is indicated and that CD7 has to indicate 35 km/h before the nozzle velocity is up to 30 km/h. The absolute comparison shows that the velocity profile is much shorter, squeezed in between the nozzle and truck front, in CD7 compared to OpR. The profiles from CD7 are cut short at -1.5 m because there the nozzle contraction starts affecting the flow, the velocity decreases, making the comparison illogical. In the open road condition this is not the case and one can clearly see, with the same line extended further out, the differences between CD7 and open road conditions. The lines do however meet nicely on the truck front at 4.5 m downstream of the nozzle. The figure also shows that inside the nozzle, at approximately -0.5 m, is a point which could allow a free-stream velocity estimate.

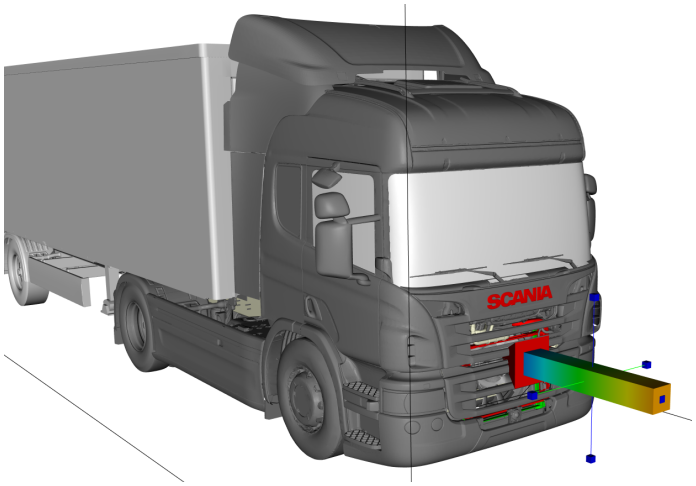

Figure 5.7: Illustration of the line measurement that is used for the velocity profile.

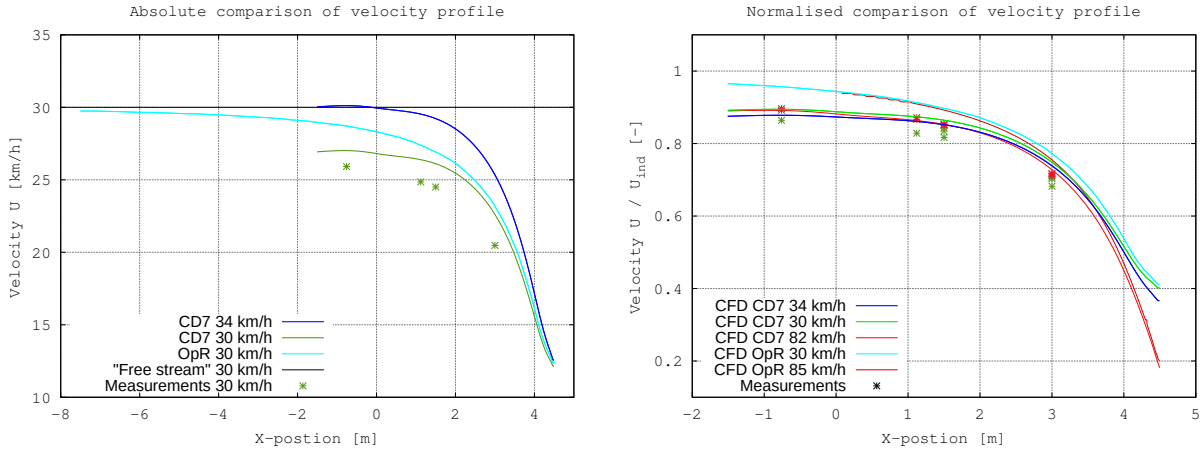

Figure 5.8: Comparison of the velocity profile along the centre line one meter above ground level in front of the truck. Absolute comparison at 30 km/h (left) and normalised comparison of all airspeeds together with measurements (right).

To the right in figure 5.8 are normalised velocity profiles so that comparisons can be made between the different airspeeds. Also included in this plot are the wind-tunnel measurements, the measurements are normalised with the indicated velocity of CD7 and so are the wind-tunnel simulations, whilst the open road cases are normalised with 30 km/h and 85 km/h respectively. The tight grouping of the measurements around and close to the CFD lines gives confidence in the simulations. This figure also shows the overestimation by CD7 of the free-stream velocity. The open road lines are both clearly extending towards 1 whilst the lines from CD7 are leveled out at 0.9, the normalisation would have removed any difference in level between these cases if the indicated airspeed was correct. It's also possible to see how the airspeed is reduced more on the front in 85 km/h (to $\approx 0.2U_{ind}$) than in 30 km/h ($0.4U_{ind}$), probably caused by the different fan speed not sucking as much air through the heat exchangers at 85 km/h.

5.5 Thermal management

The general behaviour of Fuego is similar on open road and in CD7 but there are some significant differences in local flow and temperature phenomena which are presented in their respective sections.

5.5.1 Temperature distributions

By plotting the temperature in similar planes the movement of hot air can be followed which also show important air flow phenomena.

30 km/h full load – Hill climbing

The flow through the engine compartment is very similar between OpR and CD7 (governed mostly by the fan at this driving condition) but the hot air from the engine is expelled differently around the front wheels and under the trailer in CD7. This is shown with the ambient temperature around the truck visualised in planes with a very tight temperature span in figure 5.9 to catch the effects in the surrounding air. In the horisontal planes (right pair in figure 5.9) one can see pockets with elevated temperatures in the front corners of CD7 but the main difference around Fuego is how the hot air is allowed to extend further out in CD7 whilst in open road the flow field is much more closed around the truck. The vertical planes (left pair in figure 5.9) show how the moving ground allows more hot air to be expelled under the truck and also beneath the trailer and up through the truck trailer gap. Also note how the temperature increase is stopped under the trailer in CD7 whilst it is drawn out by the road in OpR, another indication of the reversed flow under the trailer in CD7.

With a higher temperature span the internal temperature field can be evaluated as well. Figure 5.10 shows a slice 1 m above the floor in, from left to right, OpR at 30 km/h then CD7 indicating 30 km/h and to the far right is CD7 indicating 35 km/h. One can clearly see the

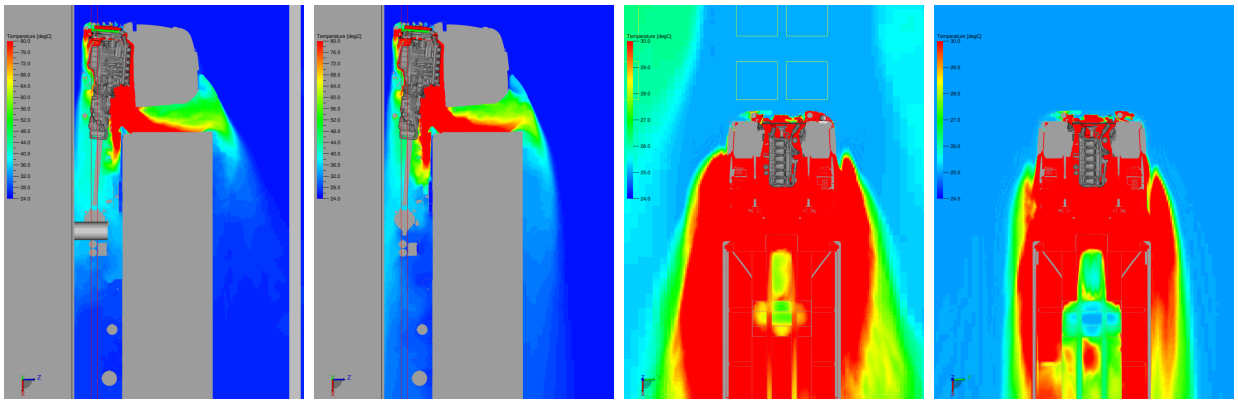

Figure 5.9: Temperature in the fluid around Fuego in CD7 (left of each pair) and on open road (right of each pair).

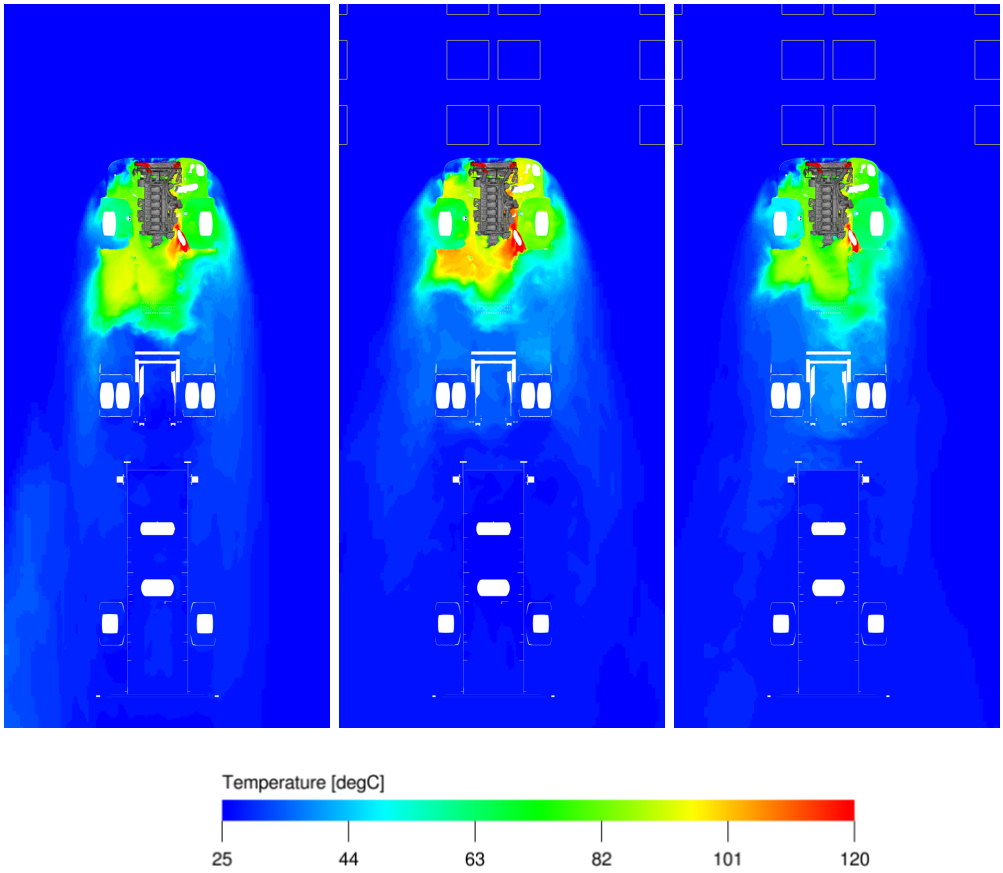

Figure 5.10: Temperature field of the fluid inside and around Fuego in OpR at 30 km/h (left) in CD7 at 30 km/h (middle) and in CD7 at 35 km/h. The slices are taken horisontally at 1 m just below the turbo and still in the wheel housing.

difference in temperature level between OpR and CD7 at 30 km/h and that they coincide better when CD7 indicates 35 km/h. The temperature perturbations are still different in CD7, most prominent is the protrusion to the left on OpR which is not found in CD7. Also visible is the increased temperature in the wheel housing especially in CD7 at 30 km/h and again how the hot air is extending further out from the truck sides.

It can also be visualised with isosurfaces as done in figure 5.11. The surfaces enclose the

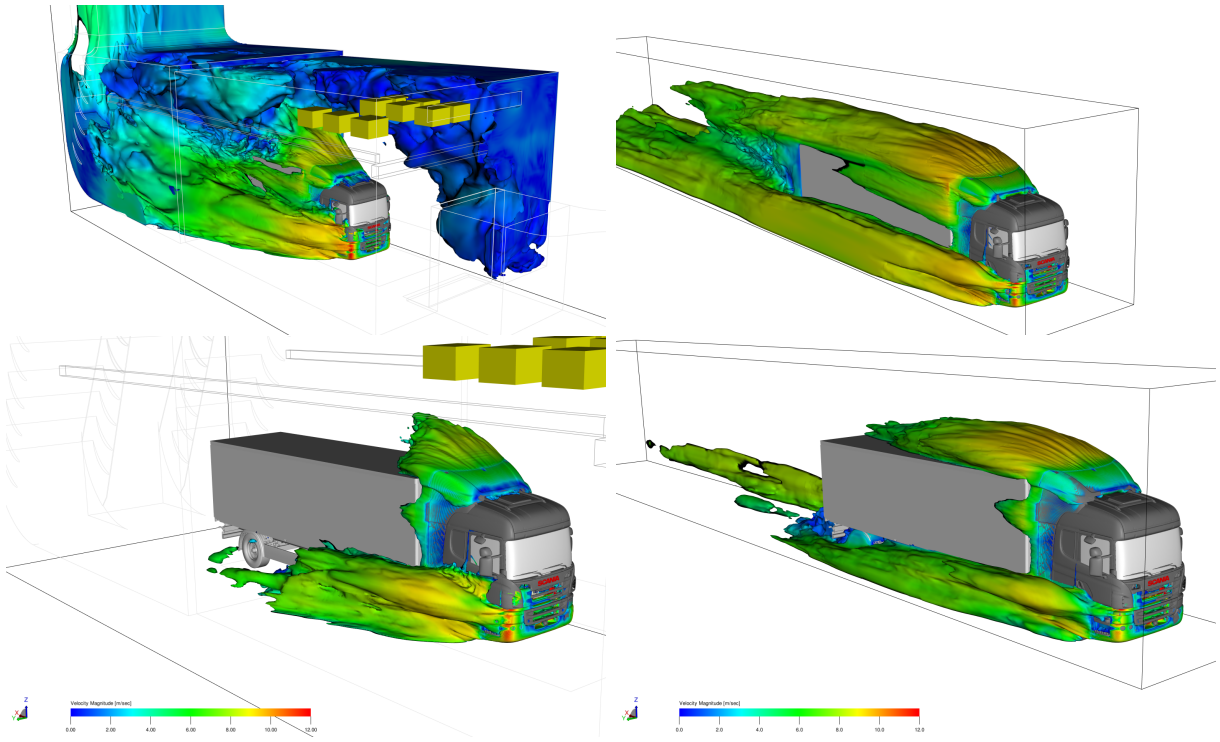

Figure 5.11: Temperature isosurfaces at 26 °C (top) and 29 °C (bottom) in the fluid around Fuego in CD7 (left) and on open road (right).

fluid with a temperature higher than 26 °C and 29 °C and the colour represents the velocity magnitude. From these figures it is possible to see an increase in ambient temperature formed in the left front corner of CD7, also a sign of the large scale recirculation inside CD7. In the iso-surface of 29 °C it can also be seen that the increased temperature around the truck extends laterally further out in CD7 but not as far back as in open road conditions.

A comparison of the defined temperature probes between open road (reference) and CD7 at the two comparable airspeeds is displayed in figure 5.12. It shows both increased and decreased temperatures in different positions. Keep in mind that these are time averages of, at some positions, oscillating temperatures due to turbulence. Therefore 1 σ, calculated from the time signal, is included as the black interval in the plots. The time signals from the thermal probes can be seen in the Appendix B.2. The recirculation probes CTL ## Pcool (especially CTL 21 which shows a large anomaly at 30 km/h) are generally better with CD7 running at 34 km/h.

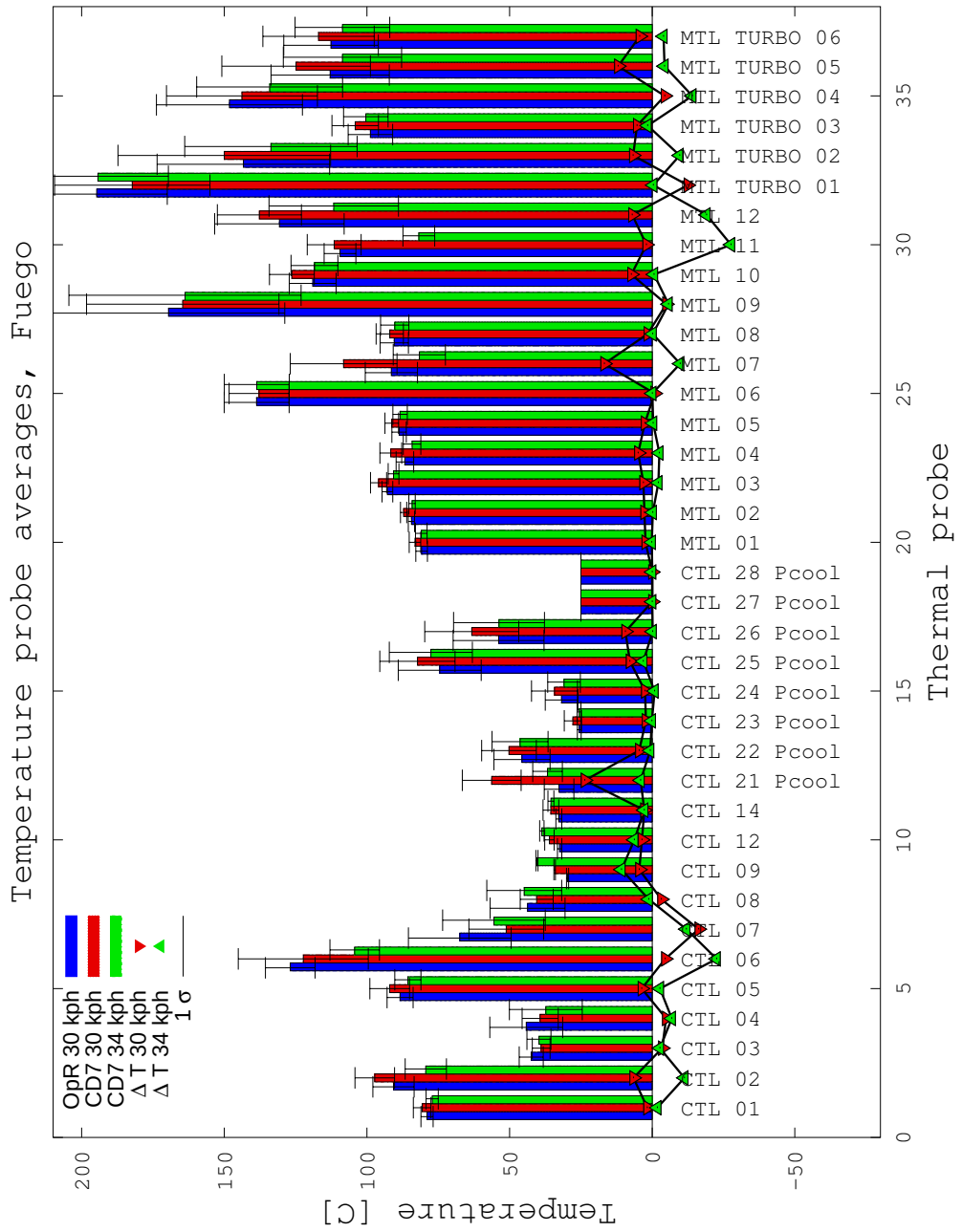

Figure 5.12: Temperature comparison of defined temperature probes.

85 km/h partial load – highway driving

In the higher speed cases the mismatch in velocity between OpR and CD7 makes the comparison inexact. The qualitative effects are still there with more hot air being expelled through the wheel houses and the reversed flow beneath the trailer that stops the hot air in that direction in CD7, see figure 5.13. When studying the isosurfaces at this higher speed, shown in figure 5.14, the wheel wake is much more compressed and the differences are much smaller. One visible difference is the volume of the iso-surface of the temperature going out from the truck trailer gap and the airspeed, given by the colour of the surface, around that region.

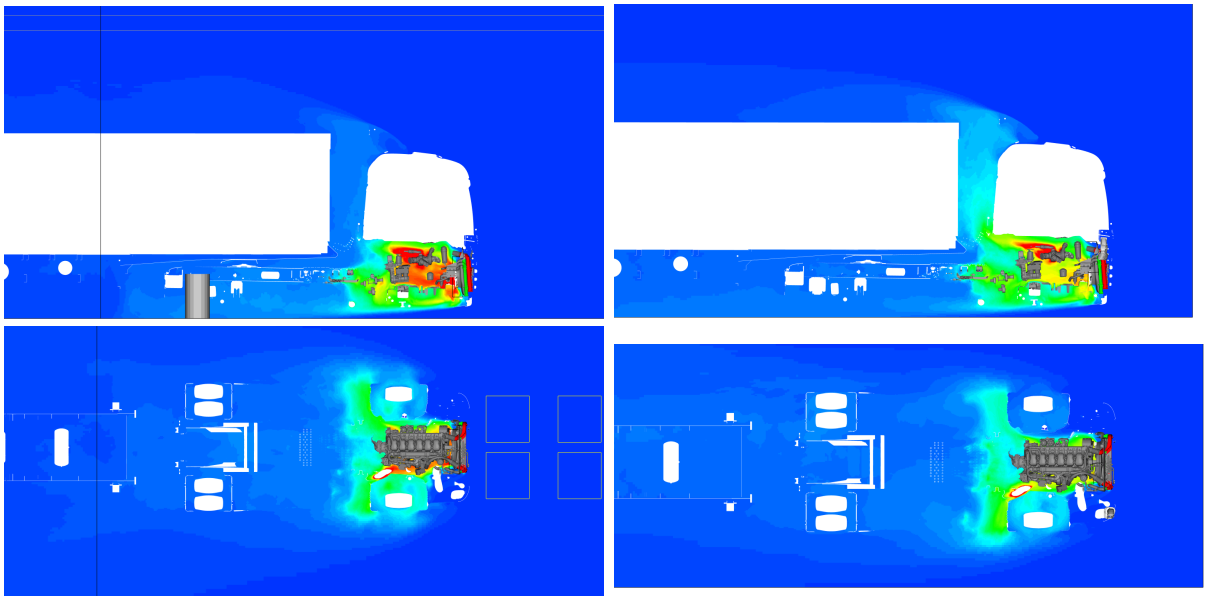

Figure 5.13: Temperature field of the fluid inside and around Fuego in CD7 (left) and on open road at 85 km/h (right). The slices are taken vertically at a 0.3 m offset from the centre line to cut the turbo (top) and horisontally at 1 m just below the turbo and still in the wheel housing (bottom).

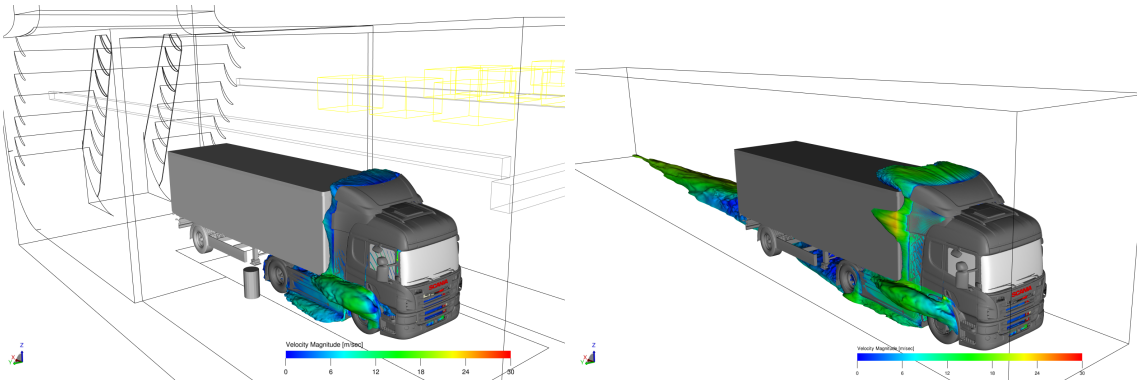

Figure 5.14: Temperature isosurfaces at 29 °C in the fluid around Fuego in CD7 (left) and on open road (right).

5.5.2 Cooling assembly

Temperatures and airflow in and around the heat exchangers have a direct effect on the cooling performance of the truck. The amount of recirculation is measured by the increase in temperature at the CAC external inlet compared to the ambient temperature and can be studied with streamlines seeded behind the fan, see figure 5.15 of the OpR case at 30 km/h. If streamlines manage to travel around and re-enter the CAC they will indicate where the leak is and here, when coloured by temperature, how hot the recirculating air is. For performance comparison the averaged temperature of the planes at the external inlet and outlet surface of the CAC and RAD are displayed in table 5.4 together with the external mass flow through the heat exchanger. The mass flow for both coolers only show small differences when the airspeed is tuned in "CD7 Fuego 1" to "3" but with the mesh refinement in "4" the mass flow

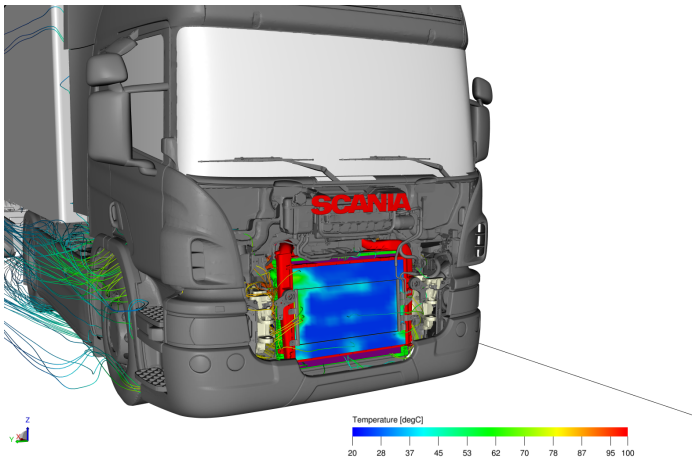

Figure 5.15: External surface temperature of the CAC and streamlines indicating recirculation.

Cooling assembly: Mass flow [kg/s], Temperature [°C]								
Case	CAC			RAD			FAI	T_{cool}
	mass	T in	T out	mass	T in	T out		
OpR Fuego 1	2.88	31.5	50.4	3.82	49.0	88.8	50.7	86.2
OpR Fuego 2	2.95	31.1	49.7	3.94	48.7	87.3	31.2	84.9
CD7 Fuego 1	2.85	32.2	51.2	3.77	50.1	90.4	53.7	87.7
CD7 Fuego 2	2.86	31.8	50.8	3.79	49.6	89.7	53.3	87.1
CD7 Fuego 3	2.87	31.9	50.8	3.79	49.7	89.7	32.4	87.1
CD7 Fuego 4	2.94	31.2	49.8	3.93	49.0	87.7	31.8	85.1
CD7 Fuego 5	2.97	30.7	49.4	3.98	48.3	86.7	31.2	84.2
CD7 Fuego 6	2.92	32.2	50.8	3.89	50.5	89.6	35.3	87.4
OpR Fuego 85	1.56	25.0	40.4	2.10	36.6	81.5	40.1	69.0
CD7 Fuego 85	1.21	25.0	44.2	1.65	39.3	95.5	42.9	83.9

Table 5.4: Simulation results of heat exchanger temperatures.

changes dramatically. Inlet and outlet temperatures are inherently linked to the mass flow but also on the airspeed dependent recirculation phenomena. At 85 km/h the recirculation effects is completely gone, as the CAC inlet temperature is equal to the ambient temperature. However, the mass flow and other temperatures are very different between the two cases, probably because of the mismatch in airspeed.

The FAI inlet temperature and cooling capacity show on high sensitivity to airspeed at 30 km/h, 3.5 °C difference in the FAI temperature and 2.3 °C in cooling capacity between the two runs in CD7.

Many of the phenomena can be accounted to the lack of ground motion and attached airflow around the truck and trailer. For instance the signs of reversed flow under the trailer in CD7 could explain the lower CTL temperatures further back on the chassis.

Chapter 6

Experimental results

In this chapter the results of the wind tunnel measurements are presented. Comparisons of the experimental data to the simulations are made. The experimental data is no way near as extensive as the simulation data but offer interesting comparisons for velocity indication and simulation verification.

6.1 Campaign

The measuring campaign was performed over three days in CD7 itself. The measurements were performed with the two pressure gauges mentioned earlier, unfortunately the data recording system failed during the campaign so the instruments had to be read manually, i.e. no transient data could be captured.

6.2 Tunnel points

The calculated airspeed was normalised with the most forward measurement point, at $x = 1.50$ m, to allow comparison between wind-tunnel measurements at different speeds and the simulations. Airspeed from the measurement points is shown together with CFD results in figure 6.1. The jet shape of the empty wind tunnel is captured well by the measurements, the points are grouped well together and close to the lines from CFD. The expansion of the jet as it enters the test section can be confirmed by the lateral points "x1-4". With the truck inside the tunnel the flow is expectedly disturbed and more turbulent. The measurements are roughly in the right place but do not display the same conformity as the measurements of the empty wind tunnel. The velocity profile in front of the truck at $y = 0$ m is captured well and the profiles further aside at $y = 2.50$ m and 3.50 m are similar but close to the truck side, at $y = 1.52$ m, the measurements are not valid. The negative values of the velocity profile in figure 6.1 are not physical velocities. The Prandtl-probe measures the dynamic pressure as a difference between the total and static pressure port but this is only valid for small yaw angles of the probe. With a negative pressure difference, the probe is not set correctly with respect to the flow field.

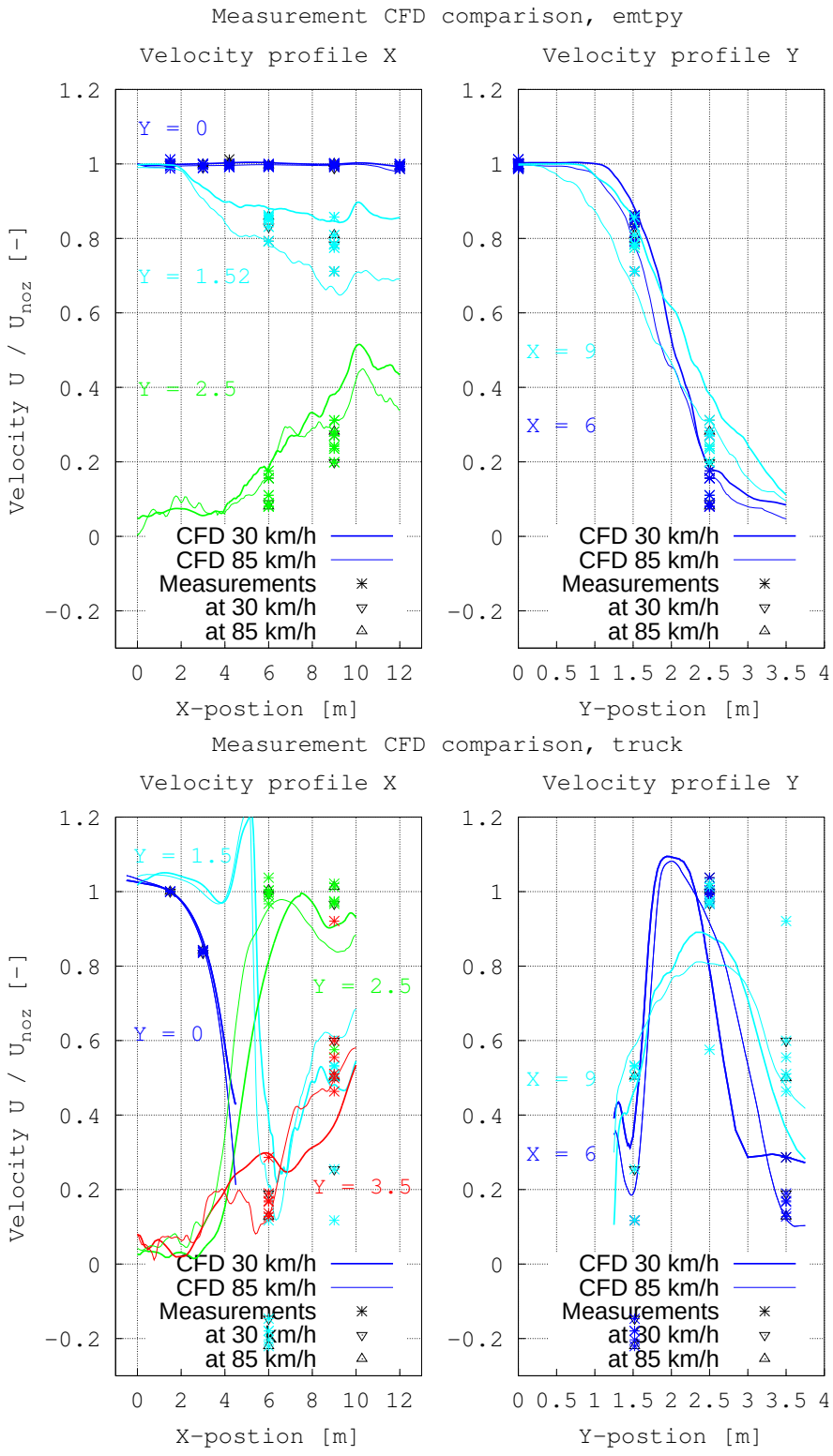

Figure 6.1: Velocity profiles of the wind tunnel jet when empty (top pair) and with truck (bottom pair). The lines represent CFD comparisons to the measurment data in stars.

The same measurements are plotted without the CFD lines and with respect to airspeed in figure A.1 of Appendix A, showing no clear difference in jet shape or behaviour discernible between the different velocities.

6.3 Surface pressure

The measured surface pressures are used to calculate pressure coefficients along the line over the surface, explained in 4.3. The c_p lines from different velocities are shown in figure 6.2, they are slightly asymmetric and have in the stagnation region on the windscreen a large offset from CFD results. On the windscreen a high pressure coefficient (reaching 1 in the stagnation point) was expected and is confirmed in CFD but was not measured in the wind tunnel. The asymmetry could arise from e.g. a small yaw angle of the truck and from the asymmetric mirror.

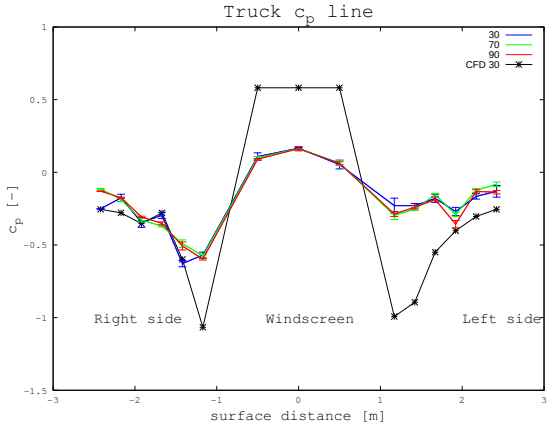

Figure 6.2: Surface pressure measurements, c_p line on truck surface at 30, 75 and 90 km/h and from CFD at 30 km/h.

6.4 Wind tunnel airspeed measurements

The indicated airspeed from the wind tunnel is compared to measured airspeed in the empty wind tunnel and with truck. In the empty wind tunnel the velocities shown in table 6.1 are taken as the average of the first three points "o1" to "o3". When multiplied with the given blockage factor the measured velocities conform better with the indicated airspeed.

According to the comparison of velocity profiles in front of the truck a measurement at x = -0.72 m is used to give a free stream velocity estimate which is compared to the indicated velocity from CD7 in table 6.2. This shows again that the wind tunnel overestimates the airspeed, on average about 12 %.

Airspeed comparison, empty [km/h]				
CD7 Indicated	Measured	Corrected	Error	Relative [%]
15	13.3	14.6	-0.4	-2.3
30	26.0	28.6	-1.4	-4.6
50	44.6	49.0	-1.0	-1.9
70	63.0	69.3	-0.7	-1.0
85	76.6	84.3	-0.7	-0.9
90	81.2	89.3	-0.7	-0.7

Table 6.1: Indicated airspeed compared to measured in empty wind tunnel.

Airspeed comparison, truck [km/h]			
CD7 Indicated	Measured	Error	Relative [%]
30	25.9	-4.1	-14
70	62.4	-7.6	-11
90	80.7	-9.3	-10

Table 6.2: Indicated airspeed compared to measured nozzle velocity in the wind tunnel with truck.

6.5 Wind tunnel systems – Blockage

To examine blockage effects the wind tunnel system parameters, fan speed and dynamic pressure, given by the control program are noted for each airspeed. They are plotted in figure 6.3 with the empty run values in blue and with Sorgenfrei in green. Lines are fitted for each set of points and the difference between these lines are plotted in red. One can then see that the wind tunnel systems hardly notice the introduction of the truck in the air stream, the difference in fan speed is less than 1 rpm. The dynamic pressure on the other hand is used to regulate the airspeed so the low difference there is good but with the blockage correction of 10 %, larger deviations of the fan speed were expected.

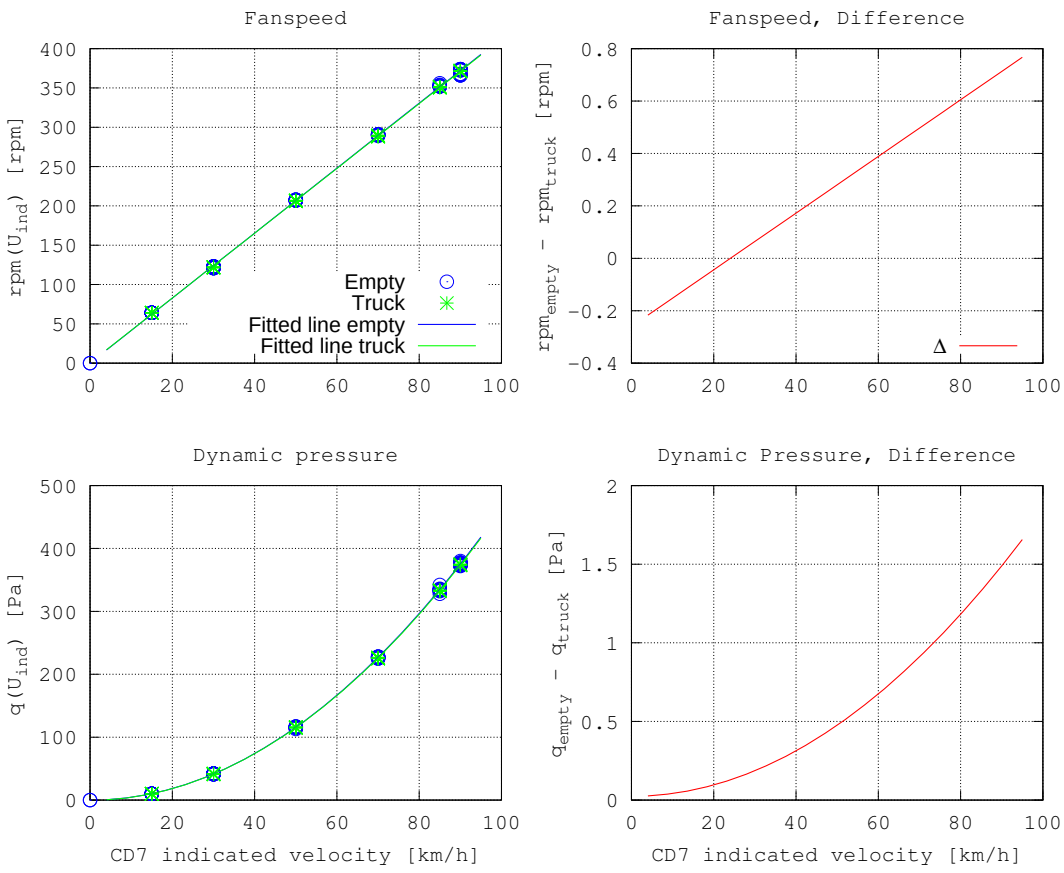

Figure 6.3: Fan speed (top pair) and dynamic pressure (bottom pair) from the wind tunnel control program. The absolute comparison of the wind tunnel system parameters (left pair) and the difference between these (right pair) show that they are not affected by the truck.

6.6 Visualisation

The visualisations described in 4.4 did not result in any hard data but some notes about the observations will be mentioned.

The one meter stick with ribbon was used to show turbulence around the mirrors and to check the flow around the measurement points. The 1.52 m points were turbulent, the 2.50 m point was visibly smoother and out at 3.50 m the airspeed was visibly weakened, confirming the results regarding the flow structure around the truck from both experiments and simulations. The stagnation point could be found just on top of the front logo.

Rain "PIV" visualisation, with the rain system and solar lamps on the water haze could be tracked optically. The large scale circulation seen in CFD was clearly visible with water haze moving forward, towards the nozzle and falling down beside the main jet.

During the soiling tests with the luminous spray around the truck it was possible to see a very strong vortex starting behind and below the door handle. This could be the wheel wake or due to the vortex generator on the cab corner.

Chapter 7

Discussion and future work

In this chapter the results and comparisons are discussed and recommendations for future work are given where applicable.

7.1 Convergence

The simulations have been run repeatedly with small changes and exhibiting similar results and some points worth mentioning are listed below.

7.1.1 Grid refinement

The first refinement scheme was given from earlier simulations at Scania. As part of good practice it was refined further in one simulation and showed differences in the truck heat exchangers and thermal probe temperatures. This would indicate that these values are not properly captured and the remaining simulations were done with the extra refinements. Thus the key comparisons in table 5.2 are all done with the same refinement definition "finer". Unfortunately when the "even finer" simulation was done the values changed further. It has been argued that the same grid refinement is enough for comparability between the simulations but making a conclusive comparison (to reality) is dangerous. When the studies continue it would be prudent to properly analyse the mesh dependency of the heat exchanger parameters.

7.1.2 Oscillations

The simulations of CD7 were subject to an oscillating phenomenon. Fortunately the oscillation was damped and after 9 s coarse simulation the amplitude had fallen below 10 Pa. The solution was then averaged over a full period of the oscillation to minimize its effect. This was deemed satisfactory for the simulations at hand, the temperatures and heat exchanger mass flow especially studied in this paper were not affected by these oscillations. This is

probably because of the flow inertia of the heat exchangers and the constrained flow through the engine compartment.

7.1.3 Wind tunnel verification

The comparison of the CFD simulations and real wind tunnel measurement that, despite the rudimentary manual data capturing, shows similar behaviour and at least (in most points) not contradicting results is reassuring. The contradicting points in the wind tunnel measurements are very close to the truck and can be explained by the highly irregular flow around the wheel wake. The low surface pressure measurements are harder to account for but the current explanation assumes that the pressure probes are unsuitable for this particular type of measurement, close to stagnation.

7.1.4 Conclusion

Thus the simulation results are treated with confidence.

7.2 Geometry

The simulations have been performed with a simplified geometry of the wind tunnel. There are a lot of possible refinements, with a number of ventilation inlets, outlets, guide vane details and so on. Horrigan *et al.* (2007) state that increased level of detail gave them better predictions of aerodynamic properties of the truck and wind tunnel configuration. However Martini *et al.* (2014) who did thermal tests state that small geometry changes of their wind tunnel had little influence on their major results. They have very different setups and goals with their studies, the first one is a scale tunnel and predictions of aerodynamic properties and the second is about full scale testing also in an aerodynamic wind tunnel but for thermal properties. No such study was done within the scope of this paper but it suggests that for the thermal tests increased refinement of the CD7 geometry would be unnecessary.

7.3 Indicated airspeed

In these simulations it is found that CD7 indicates a higher airspeed than experienced by the truck when compared to open road. To achieve the same dynamic pressure, q_{est}, on the truck as 30 km/h open road, CD7 should indicate closer to 35 km/h. Heat exchanger mass flow and temperatures also support this claim but amongst the thermal probes this is not as clear. The recirculation probes "Pcool" compare better at 35 km/h whilst some of the chassis and engine probes are closer at 30 km/h.

In the comparison of the velocity profile in front of the truck 5.4.2 the CFD result shows that at -0.5 m, inside the nozzle, the dynamic pressure is close to free stream conditions at open road. There are however a lot of other phenomena in this region, airspeed, BLRS and truck size that could change the position and character of this point. If the nozzle velocity

is deemed a good measure of the free stream velocity the calibration could be done with the Prandtl-probe in the nozzle instead and with a reference truck inside the wind-tunnel, completely removing the CFD based blockage correction.

Both the simulations and experiments show results that question the blockage correction factor of the airspeed indication system.

The simulated airspeed indication have been calculated with calibration coefficients from the October 2012 calibration report JACOBS (2012a). Later calibrations may have changed these but at least the linear part coincide well with the κ calculated in 2.3.1. Their slightly lower values could be explained through boundary-layer effects. The offset $b = -9.98$ presented in the same section is very large for the nozzle method, it translates to 3 km/h at 30 km/h and to 1 km/h at 85 km/h and can by itself explain the difference between the two methods shown here. With the two velocities of this study the basis for a calibration from simulation results is rather weak but completely possible and could offer a better comparison between the two methods.

7.4 Thermal

Between open road and CD7 the temperature behaviour is roughly the same through the engine compartment but with some different temperature perturbations. In open road the moving ground helps ejecting the hot air backwards under the trailer whereas in CD7 reversed flow under the trailer stops this effect which can explain the lower temperature in the rear part of the chassis.

Recirculation of hot air from the engine compartment into the cooler assembly (elevated temperatures on "Pcool" in CD7) is reduced when the estimated truck dynamic pressure in CD7 is matched to the dynamic pressure of open road conditions.

The calculations of 85 km/h could not be tuned to correct airspeed due to time constraints and do not offer relevant comparisons and were therefore left out of any deeper thermal analysis.

7.5 Experiments

7.5.1 Flow character

The comparison between CFD and measurements of the empty wind-tunnel showed good conformity. This gives confidence in the general flow behaviour of the CFD simulations and its relevance for these cases. With the truck, the flow got expectedly more turbulent and higher resolution (more measurement points) with proper data recording and averaging would be required to produce good measurements for comparison. Still the levels are similar between CFD and measurements.

The solar array was set in a different, more compact setting during the experiment. In this position this is not believed to change the character of the wind tunnel in any dramatic way, the airspeed is very low in the ceiling region. Neither is the BLRS outlet above the nozzle

expected to produce any sizable change, because of the large cross section the outlet airspeed is low. However the BLRS suction inlet do make a difference, clearly visible in simulations of the empty wind tunnel. Also worth to point out is that in the real wind tunnel, with the suction off, air still passes through the system driven by the nozzle flow. The available scoop covers has to be put in for the real wind-tunnel to conform to the simulation set up of the mass flow completely off. This is not evaluated further here.

7.5.2 Surface pressures

The c_p line calculated from surface pressure measurements shows similar behaviour on the truck sides with a negative value increasing to zero but the expected high pressure region on the windscreen obtained from CFD could not be seen in the measurements. Total stagnation is not expected since the probes are located on the windscreen, above the stagnation point but the measured values are much too small. Since something close to stagnation is expected it is suspected that the measurements are bad and time constraints did not allow further investigation of this. The most accepted explanation is that the pressure probes were badly suited for the type of measurements close to stagnation but this is subject to further study.

7.5.3 Wind tunnel systems

The comparison of wind tunnel systems showed that the wind-tunnel main fan did not notice whether or not there was a truck inside. With the blockage a truck represents, an increase of fan speed was expected and its absence again question the need for a blockage correction.

Acknowledgements

I wish to extend my gratitude to Mattias Chevalier who supervised the work at Scania.

Special thanks also goes out to David Söderblom, who supervised the parallel master thesis, for his involvement and supervision in the wind tunnel campaign.

I also give my thanks to my colleague Tobias Persson who did the parallel project and sat back to back with me, always interested in discussing our results offering valuable insights during the whole project.

Big thanks to the rest of the team at RTGF at Scania, to the wind tunnel operating crew and the other people involved in the wind tunnel campaign.

Bibliography

Chen, S. & Doolen, G. 1998 Lattice Boltzmann method for fluid flows. *Annual Review of Fluid Mechanics, Vol **30**, p. 329–364.*

Cyr, S., Ih, K.-D. & Park, S. H. 2011 Accurate reproduction of wind tunnel results with CFD. *SAE International, SAE Technical Paper 2011–01–0158.*

Duell, E. & et.al., P. E. 2016 Scania's new CD7 climatic wind tunnel facility for heavy trucks and buses. *SAE Journal of Passenger cars - Mechanical systems, Vol **9**(2), p. 785-799.*

Ekman, P. & Larsson, N. 2015 Design optimisation of fan ring exit guide vanes using CFD to improve cooling capacity of heavy trucks. *Master thesis project, LIU.*

Exa 2016 The technology behind powerflow: Exa's lattice Boltzmann-based physics. Webpage: www.exa.com/company/core_technology.

Horrigan, K., Duncan, B., Sivakumar, P., Gupta, A. & Wong, A. 2007 Aerodynamic simulations of a class 8 heavy truck: Comparison to wind tunnel results and investigation of blockage influences. *Journal of Commercial Vehicles, SAE Technical Paper 2007–01–4295.*

Hyvärinen, A. 2015 Investigation of blockage correction methods for full-scale wind tunnel testing of trucks. *Master thesis project, KTH.*

Hällqvist, T. 2009 The cooling airflow of heavy trucks - a parametric study. *SAE International Journal of Commercial Vehicles, Vol **1**(1), p. 119–133.*

I-010, J. 2013 Jacobs drawing, I-010. *Confidential internal document.*

Inamuro, T. 2006 Lattice Boltzmann methods for viscous fluid flows and two-phase fluid flows. *Fluid Dynamics Research, Vol **38**(9), p. 641–659.*

JACOBS 2012a Airspeed calibration report. *Confidential internal report.*

JACOBS 2012b Boundary layer system calibration. *Confidential internal report.*

JACOBS 2012c Jacobs aero thermal test plan. *Confidential internal report.*

Martini, H., Gullberg, P. & Lofdahl, L. 2014 Comparative studies between CFD and wind tunnel measurements of cooling preformance and external aerodynamics for a heavy truck. *Journal of Commercial Vehicles, Vol* ***7****(2), p. 640–652.*

Mohamad, A. 2011 *Lattice Boltzmann Method.* Springer.

Persson, T. 2016 Wind tunnel effects on truck aerodynamics and soiling. *Master thesis project, KTH.*

Tarnutzer, T. 2013 Final documentation overview. *Confidential internal report Scania CV.*

Appendix A

Wind tunnel measurements

A.1 Measurement points

The Prandtl probe positions in CD7 experiments are defined in table A.1.

Point	Measured	x [m]	y [m]	z [m]
o1	both	1.50	0.00	1.00
o2	both	3.00	0.00	1.00
o3	both	4.20	0.00	1.00
o4	empty	6.00	0.00	1.00
o5	empty	9.00	0.00	1.00
o6	empty	12.0	0.00	1.00
x1	both	6.00	1.52	1.00
x2	both	6.00	2.50	1.00
x3	both	9.00	1.52	1.00
x4	both	9.00	2.50	1.00
x5	truck	6.00	3.50	1.00
x6	truck	9.00	3.50	1.00

Table A.1: Definition of measurement points in CD7.

A.1.1 Velocity measurements

To check for velocity dependent differences of the jet, the velocity measurements are plotted together and normalised with the most forward point, o1, see figure A.1. The lines are colour coded, green is slow, 15 km/h and when faster shifts towards red, 90 km/h. This is the same data as in figure 6.1 therefore the negative velocities are here also not physical.

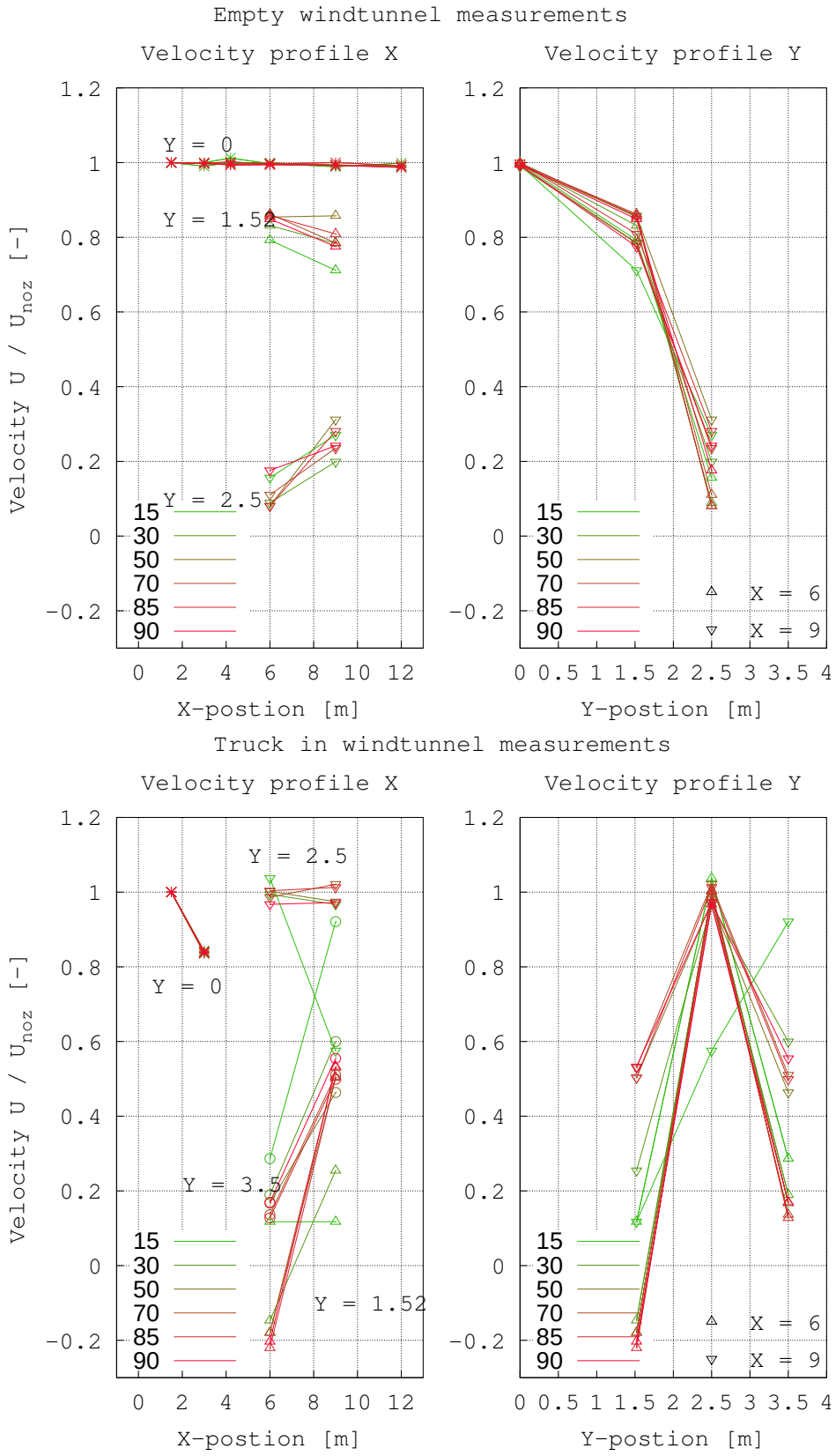

Figure A.1: Measurement points in wind tunnel with and without truck.

Appendix B

Temperature aspects

B.1 Heat exchangers

Comparison of heat exchanger properties. The time signals level out very quickly but the mesh dependency is clearly visible in figures B.1. The "even finer" refinement was only done for the CD7 simulation to verify convergence and was not used in any deeper analysis.

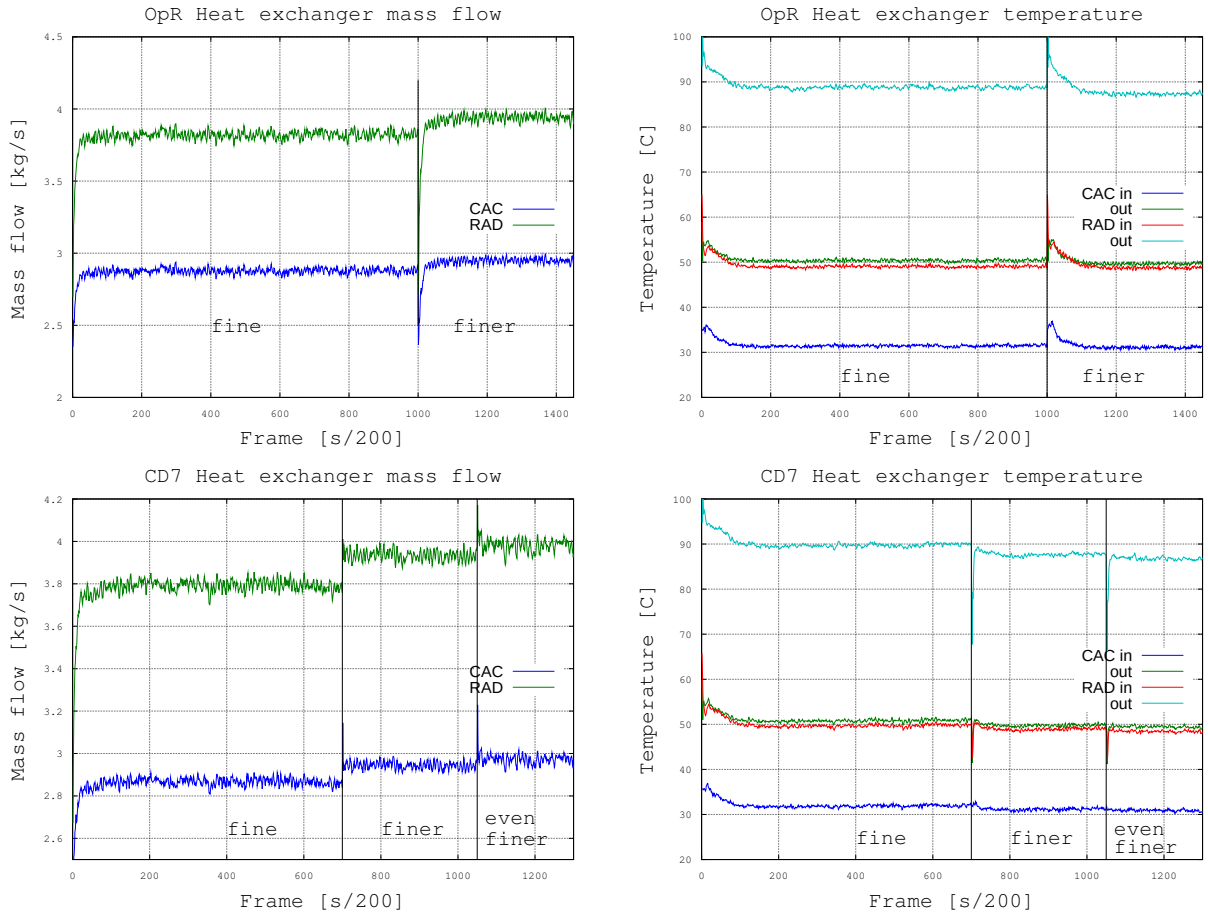

Figure B.1: Convergence analysis of truck parameters, heat exchanger external mass flow (left) and external temperatures (right) for both OpR conditions (top) and in CD7 (bottom).

B.2 Temperature probes - time signals

The recorded time signal of temperature probes are shown in figures B.2, B.3 and B.4. CTL denote the chassis probes, Pcool the recirculation probes on the cooling assembly, MTL the probes around the engine and TURBO the probes around the turbo installation, defined in figure 3.6.

Some probe signals converge very quickly to a steady state, MTL 01 and 08 on the front of the engine, whilst some oscillate violently due to turbulence e.g. CTL 6 next to the silencer and Pcool CTL 25 and 26 due to recirculation around the cooling assembly.

Open road

Thermal probes, open road reference.

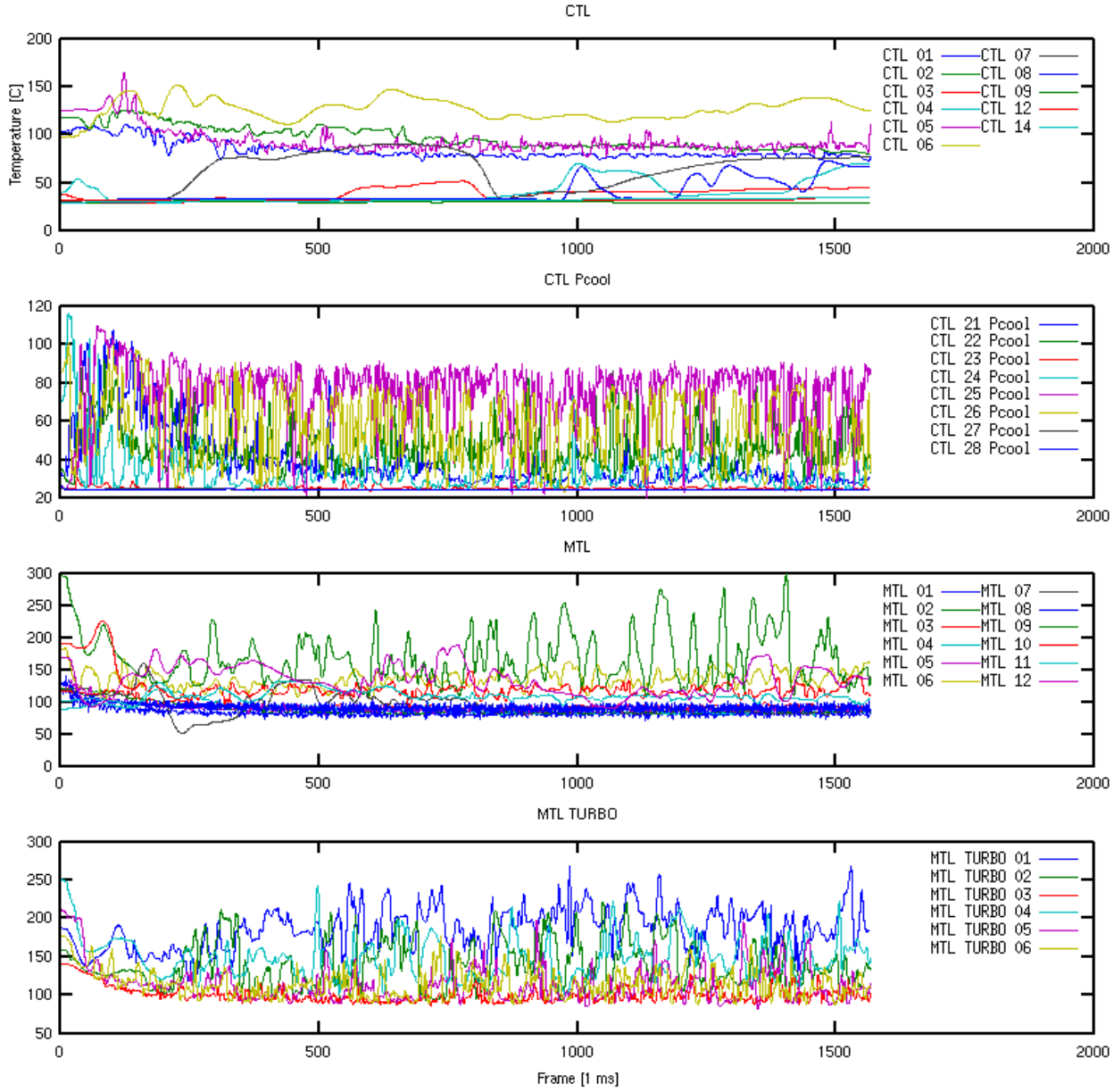

Figure B.2: Time signals of the temperature probes on Fuego in open road conditions. The chassis- "CTL", recirculation- "P cool", engine- "MTL" and turbo- "TURBO" probes are separated in subplots.

CD7 - native

Same measurements from the CD7 simulation at 30 km/h indicated.

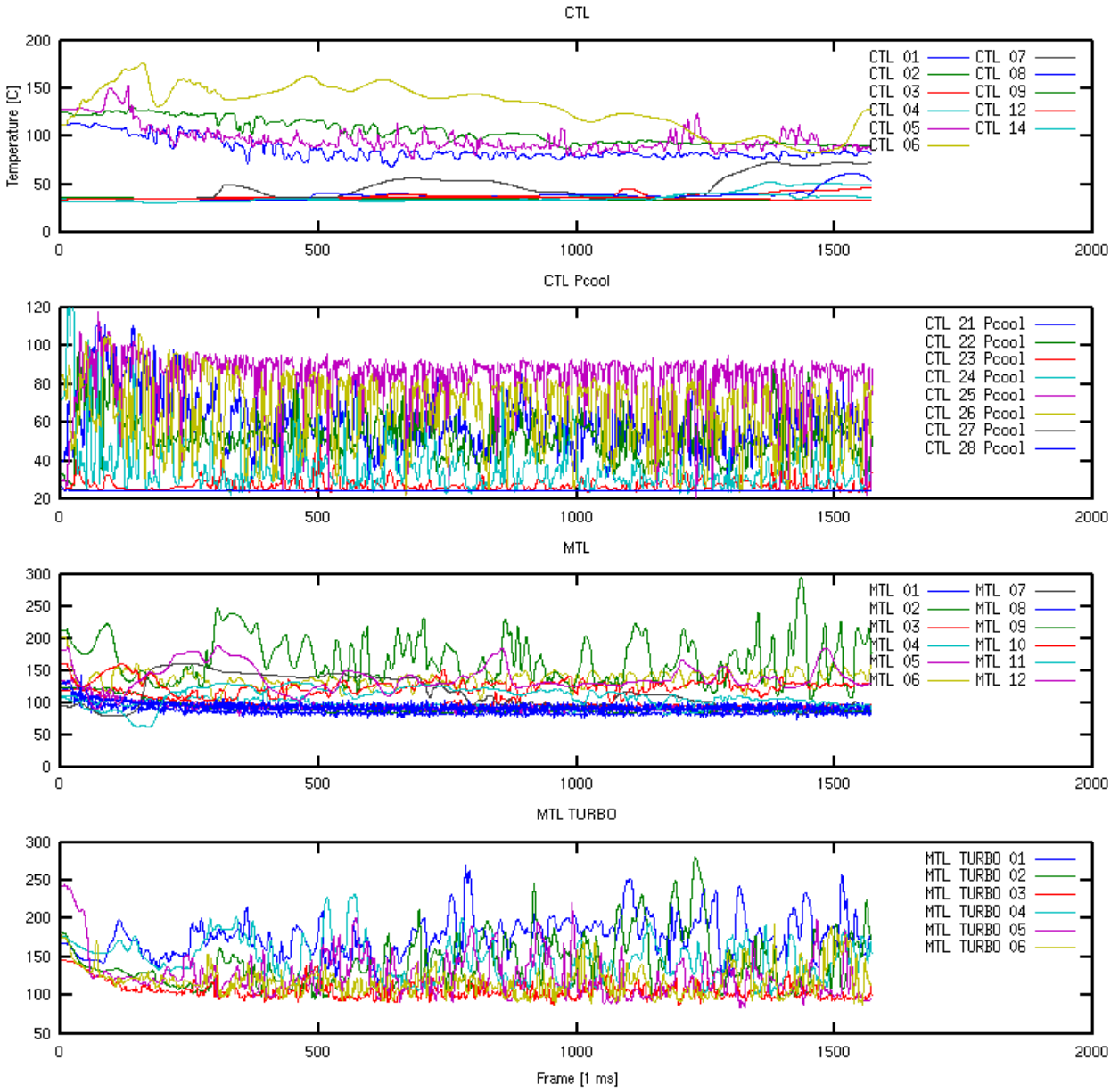

Figure B.3: Time signals of the temperature probes on Fuego in CD7 indicating 30 km/h. The chassis- "CTL", recirculation- "P cool", engine- "MTL" and turbo- "TURBO" probes are separated in subplots.

CD7 - tuned

Same measurements from the CD7 simulations at 35 km/h indicated.

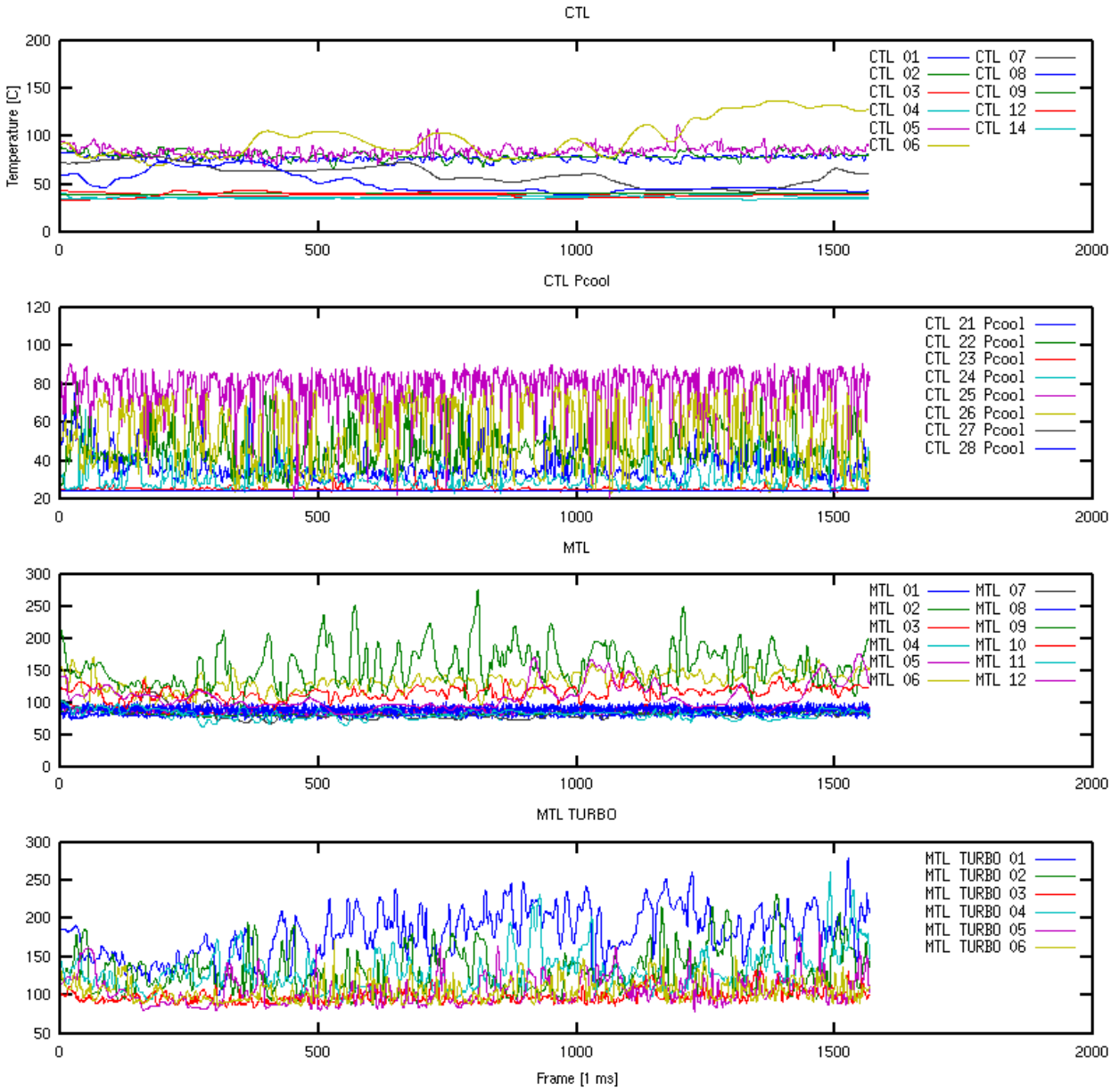

Figure B.4: Time signals of the temperature probes on Fuego in CD7 indicating 35 km/h. The chassis- "CTL", recirculation- "P cool", engine- "MTL" and turbo- "TURBO" probes are separated in subplots.